

GPO PRICE \$ _____
 CFSTI PRICE(S) \$ _____
 Hard copy (HC) \$3.00
 Microfiche (MF) 1.75

7 653 July 85

FACILITY FORM 802

N66 27209
 (ACCESSION NUMBER)
 66
 (PAGES)
 TMX - 56605
 (NASA CR OR TMX OR AD NUMBER)

(THRU)
 (CODE) 29
 (CATEGORY)

OBSERVATIONS OF THE SOLAR WIND

DURING THE FLIGHT OF IMP-I

by

John H. Wolfe

Richard W. Silva

Marilyn A. Myers

National Aeronautics and Space Administration

Ames Research Center, Space Sciences Division

Moffett Field, California

[REDACTED]

ABSTRACT

27209

Some of the principal results of an experiment designed to investigate the properties of the solar wind and its interaction with the geomagnetic field are discussed. The main objective of the experiment was to measure the energy per unit charge and gross flow characteristics of the positive ion component of the incident plasma as a function of radial distance from the earth. This experiment was carried out on the IMP-I (Explorer 18) spacecraft using a curved plate electrostatic analyzer.

The satellite was launched from Cape Kennedy into a highly eccentric orbit of about 31 earth radii apogee on November 26, 1963, with an initial sun-earth-apogee angle of approximately 27° in the dawn hemisphere. Plasma observations indicate that three distinct regions of space were traversed by the satellite. The first was the geomagnetic cavity where no plasma was observed within the dynamic range of the instrument. The second was the region of turbulent plasma flow associated with the interaction between the solar wind and the geomagnetic field. The third was interplanetary space where the free streaming solar wind was observed. The results presented cover the first 2-1/2 months of satellite life.

The plasma data obtained in interplanetary space revealed that the solar wind density rarely exceeded 3 ions cm^{-3} . The free-stream

velocity exhibited values from less than 300 km/sec during quiet times to more than 700 km/sec at the time of geomagnetic disturbances.

Observations in the transition region consistently showed a large increase in the entropy of the plasma as compared to interplanetary space. Careful examination of the change in the plasma characteristics as the spacecraft passed through this region has allowed the extremities of the transition region boundaries to be extensively mapped. The data revealed that toward the subsolar point the outer boundary of the transition region was located some 4 to 5 earth radii upstream from the magnetospheric boundary and showed increasing standoff distance with increasing angle from the earth-sun line. The geomagnetic cavity was seen to flare out from the subsolar point running approximately parallel to the earth-sun line for angles greater than about 130° to 140° from the subsolar point. No indication of closure of the tail of the magnetosphere was observed. The transition region observations are discussed in light of present theory.

I. INTRODUCTION

Experiments on a number of satellites and deep space probes launched since 1958 have shown that the geomagnetic field extends on the sunlit side of the earth to distances of some 8 to 12 earth radii and on the night side of the earth to considerably farther distances. Measurements made by these earlier spacecraft revealed not only the boundary of the geomagnetic field but also indicated the considerable complexity of the termination process.

Although telemetry interruptions for command purposes precluded a comprehensive view being obtained from the Pioneer 1 [Sonett, 1959] and Pioneer 5 [Coleman, 1964] magnetometers, these early experiments did establish the existence of the geomagnetic field termination. These findings were subsequently confirmed by the Explorer 12 magnetometer experiment of Cahill and Amazeen [1963]. They reported the location and some of the general magnetic characteristics of the geomagnetic boundary on several satellite passes in the earth's sunlit hemisphere. The observations made by Explorer 10 on the night side of the earth [Heppner et al. 1963; Bonetti et al. 1963] established the great radial extent of the earth's magnetosphere in the antisolar direction. The above observations, together with the interplanetary solar wind measurements of Neugebauer and Snyder [1962] on Mariner 2, have established some of the general characteristics of the boundary of the earth's magnetosphere. During the time preceding the flight of IMP-I, however, observations of the plasma characteristics in the boundary region on a routine long term basis had not been made.

The plan of this paper is to discuss, in light of the IMP-I results, the extension of these earlier findings and, specifically, to describe some of the principal results of the NASA/Ames Plasma Probe experiment during the first 33 orbits of this satellite. Observations in the region of transition between the solar wind and the geomagnetic field are emphasized.

The paper considers first the experimental arrangement including the geometrical properties of the plasma probe, the procedure for data acquisition, and the pertinent spacecraft orbital and orientation parameters. This is followed by the observations, which are most conveniently divided into two parts. The first deals with a brief description of the interplanetary observations of the solar wind outside the transition region. The second concerns a more extensive discussion of the properties of the plasma subsequent to its passage through what sometimes appeared to be a shock-like boundary. The latter was identified with the transition region itself where generally an increase in the disorder of the plasma appeared to have taken place. Lastly, we discuss the experimental results and some of the implications of the data.

II. EXPERIMENTAL ARRANGEMENT

1. Instrumentation

The instrument, shown schematically in Figure 1, was a curved plate electrostatic probe designed to detect and analyze the positive ion component of the incident plasma. The ambient plasma can be considered as incident at its streaming or bulk velocity on the aperture of the probe. Although the spacecraft was translating in space, the probe velocity was unimportant compared to the plasma velocity. Behind the 0.5 cm^2 aperture were mounted two concentric quadrispherical analyzer plates. Beyond the exit aperture of these plates was a collector maintained at approximately spacecraft ground potential. A 14-step cyclic staircase voltage, shown in Figure 2,

Fig. 1

Fig. 2

was applied across the analyzer plates and the positive ion current to the collector was measured and recorded as a function of the instantaneous plate voltage, V_a . It can be shown that the curved path of a particular ion passing between the analyzer plates was primarily a function of the energy per unit charge of the ion and the analyzer plate voltage difference, V_a , with a second-order dependence on the angle of incidence of the ion with respect to the entrance aperture. Thus the analysis system was inherently differential and only those incident ions in a narrow band centered about some mean value of energy per unit charge, corresponding to a particular plate voltage, passed through the analyzer to the collector. The mean radius of curvature of the analyzer plates was 3.0 cm with a separation of 0.25 cm. This yielded an analyzer constant of approximately 6, where the analyzer constant is defined by the equation $E/Q = 6 V_a$, where E/Q is the energy per unit charge of the ion accepted for an analyzer plate potential difference of V_a .


The instrument had a sensitivity range for singly charged positive ions from approximately 3×10^5 to 1×10^{10} ions $\text{cm}^{-2} \text{sec}^{-1}$ over a range of energy from approximately 0.025 to 16 kev. The energy resolution, defined by $\Delta E/E$, was slightly energy dependent varying from a full width at half maximum value of 6.5% to 8.5% over the full energy range of the instrument.

The resulting ion collector current was amplified by a subminiature electrometer tube and feedback circuit which produced an extremely high input impedance and a logarithmic response. The

amplifier circuit had a threshold sensitivity of 10^{-14} ampere, a dynamic range of approximately 10^4 , and a response time of about 0.1 second.

Sensitivity to solar ultraviolet was eliminated by blackening the analyzer plates. The blackened plates together with their inherent curvature constituted an effective deterrent to the production of photoelectrons along either the exit region of the analyzer plates in the vicinity of the collector or on the collector itself. Primary electrons in the solar wind or in the more disordered gas of the transition region are effectively excluded from the collector region by the rejection properties of the analyzer system. Extensive testing with ultraviolet sources has shown that the photoelectron contribution to the collector current was negligible. This was subsequently verified by examination of the flight data.

2. Analyzer Geometry and Orientation

The basic configuration of the plasma probe is shown in Figure 3.  Fig. 3
The direction of a beam of ions which enter the instrument aperture and are subsequently analyzed by the plasma probe is, for convenience, resolved into the angular components θ and ϕ . The angles θ and ϕ correspond to the polar and azimuthal angles in spacecraft coordinates. The angular component along the direction ϕ can vary over a large range of values while the θ component is restricted to a relatively small range. The electrostatic field between the analyzer plates exerts a force approximately equal to $-K/r^2$. The constant, K , is dependent on the sensor geometry and analyzer plate voltage and is given by the relation:

$$K = q \left(\frac{R_1 R_0}{R_0 - R_1} \right) V_a$$

where R_1 and R_0 are the inner and outer analyzer plate radii, V_a is the analyzer voltage, and q is the charge of the incident particle.

Since the electrostatic field is a central force field, a particle has an elliptical path through the instrument and is confined to the plane containing the initial velocity vector at the entrance and the geometric center of the analyzer plates. The small separation (0.25 cm) between the analyzer plates constrains the allowed values of eccentricity of the particle orbits to a small range and thus limits the θ acceptance to a narrow band of values. Since the eccentricity is a function of the particle energy, the energy range for allowed orbits is necessarily small. The ϕ angle is only limited by the angular size of the analyzer plates themselves (90° for quadrispheres). Thus the ϕ angular acceptance is ideally 90° . The fringing electric fields at the aperture and at the analyzer plate exit do not alter these acceptances appreciably. The exact instrument response to incident angle was determined during pre-flight calibration with a monoenergetic helium ion beam. The IMP-I instrument calibration provided a set of angular acceptance curves that revealed an instrument response which had a first-order dependence on angle of incidence, as was predicted by the above discussion, and had a second-order dependence on energy, as would be expected from the effects of finite plate separation. These angular acceptance curves have shown that the full width at half maximum angular acceptances varied from 74° to 86° for the ϕ acceptance and from

13° to 18° for the θ acceptance over the energy range of the instrument. Figure 4 shows a typical acceptance curve obtained during the preflight ion accelerator calibration with, in this particular case, θ set equal to 0° and a beam potential of 600 volts (energy step 13 of the plasma probe).

Fig. 4

The instrument was mounted in the spinning IMP-I satellite so that the angle φ was measured in the polar plane containing the vehicle spin axis and the instrument normal was perpendicular to the spin axis. The φ angular view was thus symmetrical above and below the spacecraft equatorial plane. The convention of measuring the φ angle was such that positive angles of φ corresponded to negative angles of colatitude in the vehicle frame of reference. With this mounting the instrument acceptance geometry swept a band approximately 90° wide around the celestial sphere with each vehicle revolution. The instantaneous acceptance fan was nominally 90° by 15° as is shown in Figure 5.

Fig. 5

The spacecraft spin axis was oriented initially with a sun-vehicle spin axis angle of 110° corresponding to a φ angle of -20° in the acceptance fan. This angle slowly varied during the IMP-I lifetime over a range $-39^\circ \leq \varphi \leq -15^\circ$ (see Figure 4).

3. Data Acquisition

The low information bit rate and the time sharing nature of the spacecraft telemetry system required that the plasma probe incorporate a means of sampling the incident ion flux as a function of energy per unit charge and store this information in an analog memory until it could be telemetered. Angular indexing in the θ plane (satellite

equator) was defined by dividing the equatorial plane of the spacecraft into three sectors using the optical aspect sensor as a reference. This division is shown in Figure 6 with the solar direction always contained in the second sector. The angular width of sectors 1 and 2 were equal and were defined by two monostable multivibrators, each with a gate length of 0.84 second. The time interval of sector 3, t_3 , was determined by the spacecraft spin period, τ , minus the sum of the other two sector gate lengths so that

Fig. 6

$$t_3 = \tau - 2(0.84) \text{ seconds}$$

Variation of the spacecraft spin rate over the lifetime of IMP-I caused the equal sectors 1 and 2 to change in angular width over a range from 110.9° to 130.0° and sector 3 from 137.9° to 99.7° .

Angular sequencing of the data acquisition from the plasma probe also required special consideration because of the very restricted bandwidth available for this experiment. The procedure was to index the probe to one sector and to complete a sweep in energy before advancing to the next sector. The amplifier-memory circuitry was of the peak reading variety and the analyzer plate potential was held fixed as the satellite completed one revolution. During this time the peak value of the plasma flux in the designated sector was read into the memory. The subsequent rotation of the spacecraft advanced the analyzer plate potential to the next voltage step and the process repeated while still locked onto the same azimuthal sector. The sweep in energy was completed in 14 revolutions of the spacecraft with subsequent readout by the telemetry followed by the sector

designation code. This same procedure was sequentially followed for the remaining two sectors and then the entire process repeated. For a spin rate of 23 rpm the complete energy scan in one sector took 36.5 seconds. The complete process of data acquisition and readout for a complete energy and angular scan cycle was determined by telemetry and required 5 minutes and 28 seconds.

4. Orbit and Orientation

IMP-I was launched from the Air Force Eastern Test Range at 0230 UT on November 27, 1963, with an initial apogee of 31.02 earth radii geocentric and an orbital period of 3.934 days. The resulting orbit had an eccentricity of 0.9376 and an inclination of 33.34° to the earth's equatorial plane. The initial sun-earth-apogee angle was approximately 27° toward the dawn side of the earth. Figure 7 shows the projections of the second orbit in both the noon meridian plane and in the equatorial plane. The arrows in Figure 7 refer to the earth-sun line in the noon meridian plane and the projection of the earth-sun line in the equatorial plane. The small open circles show the equatorial projections of the positions of apogee for successive orbits in terms of orbit number and date for the first 17 orbits. For the period covered in this report the sun-earth-apogee angle increased from the initial value of 27° back to 153° in the dawn hemisphere for the thirty-third orbit.

Fig. 7

The celestial coordinates of the spacecraft spin vector were 116.8° right ascension and -23.2° declination. This orientation produced at launch a spin axis-sun angle of 110° . In solar oriented ecliptic

coordinates the spacecraft spin axis was pointing approximately 44° below the ecliptic and, as viewed from the north ecliptic pole, the projection of the spin vector in the ecliptic plane made an angle of 239° measured counterclockwise from the spacecraft sun line. The plane of symmetry of the plasma probe scan was the plane normal to the spin axis, i.e., the spacecraft equatorial plane.

III. EXPERIMENTAL RESULTS

The results obtained from IMP-I lead to a natural division of space traversed by the spacecraft into three distinct regions as observed in a fixed earth-sun coordinate system. The first region corresponds to that portion of space surrounding the earth within which the solar wind confines the ordered geomagnetic field [Parker, 1959] and which contains, in the sunlit hemisphere at least, a fairly well-defined high energy charged particle trapping region [Frank et al., 1963]. The second region is defined by the region of transition between the boundary of the magnetosphere and interplanetary space, and the third corresponds to interplanetary space.

The plasma data obtained in interplanetary space indicated a relatively uniform plasma velocity compared to data obtained in the transition region where the flow was usually much more turbulent. The experimental results which follow are presented first for interplanetary space during both quiet and magnetically disturbed times and then for the transition region. The interplanetary data are reported only in terms of the gross features and characteristics that are essential for interpreting the transition region data

which, in turn, are covered in greater detail. A more extensive report of the interplanetary results and the correlation of these results with solar and geophysical phenomena is now in preparation.

1. Interplanetary Observations

Of the 33 orbits for which data are reported here, only during portions of the first 21 orbits did the spacecraft, with reasonable certainty, penetrate the space beyond the transition region. During these first 21 orbits the spacecraft was beyond the transition region for a total time of approximately 1,396 hours. During this time period plasma was observed for a total of 961 hours or 68.9% of the time. For the time when plasma was not observed, it is most likely that the occasional decrease of flux below threshold was due to the velocity and temperature of the solar wind being such that the energy spectrum fell between the energy/unit charge windows of the plasma probe. It seems clear that the almost continuous observation of plasma by the Mariner 2 plasma probe [Neugebauer and Snyder, 1962], which apparently had broader energy coverage than the IMP-I instrument discussed here, indicates that the vanishing of flux in interplanetary space observed on IMP-I was not due simply to the decrease of solar wind flux below the sensitivity of the plasma probe.

The flux and velocity of solar plasma observed beyond the transition region ranged in general from 10^6 to 10^7 ions $\text{cm}^{-2} \text{sec}^{-1}$ per energy channel ($\Delta E/E \sim 8\%$) and from less than 300 to less than 570 km/sec during relatively quiet periods. During disturbed times the flux and velocity generally ranged from 10^7 to 10^8 ions $\text{cm}^{-2} \text{sec}^{-1}$

per energy channel and from 570 to 750 km/sec. The average interplanetary solar wind velocity observed on IMP-I during the period covered by this report was 378 km/sec. If the small $\Delta E/E$ for this instrument is taken into account, the above values are in general agreement with the total positive ion flux ranges reported by Gringauz [1961] during the Lunik 2 and Venus Probe flights in September 1959, and February 1961, respectively. They are also in general agreement with the total fluxes and velocities given by Neugebauer and Snyder [1962] from the plasma observations during the flight of Mariner 2 and the observations of Wolfe and Silva [1964] on Explorer 14 during the October 7, 1962 storm.

Figure 8 shows the plasma probe data obtained during the second outbound pass of the spacecraft. In this particular orbit the line of apsides was approximately 31° from the subsolar point toward the dawn side of the earth. The ion current over the range from 10^{-14} to 10^{-12} ampere for the four lowest analyzer voltage steps is plotted as a function of the geocentric distance in earth radii and universal time. The observed ion current is approximately proportional to the incident ion flux. For a normal incidence parallel beam in the 600-volt channel, 10^{-14} ampere corresponds to approximately 3×10^5 protons $\text{cm}^{-2} \text{ sec}^{-1}$. Only the four lowest voltage levels are plotted since ion current was infrequently observed in the channels above 3740 volts (846 km/sec for protons), particularly in interplanetary space. The ion current observed in the three sectors of rotation have been plotted and are identified by the legend. Recall from Figure 6 that sector 2 contained the probe-sun line.

Fig. 8

In the second outbound pass, plasma was first observed between 10 and 11 earth radii as indicated by the appearance of ion current in all of the four lowest energy channels. Then, between 15 and 16 earth radii there was a definite shift of flux to only the 600-volt channel with the majority of flux appearing in sector 2 which contained the solar direction. There was, however, a small but finite flux in sector 1. For this orbit sector 1 viewed an angular sweep from approximately 67° to 179° measured counterclockwise from the solar direction as viewed looking down on the spacecraft spin axis. Except when near perigee, sector 1 included the probe-earth direction and thus seems to indicate the arrival of a low level flux of approximately solar wind velocity from the general direction of earth. It is important to note that the sudden shift of the bulk of the flux from the 600-volt to the 1700-volt channel at 0400 UT on December 2, 1963 (Figure 8) was accompanied by a corresponding shift of the flux in sector 1 providing confidence in the validity of this measurement. Note also the almost complete lack of flux in sector 3. Careful examination of this sector 1 current indicates that it was most likely caused by the 0.1 second time constant of the amplifier. The direction of rotation of the spacecraft dictated the scan of sector 1 subsequent to the scan of sector 2. It therefore was quite probable that the relatively high voltage signals developed by the amplifier, as a result of the high ion fluxes incident from the general direction of the sun (sector 2), would not have completely decayed to zero at the beginning of the scan in sector 1. Since the circuit is peak reading it would have reported

this residual voltage as the peak current in sector 1, provided no higher ion flux was observed during the actual scan in the remainder of sector 1.

At 2113 UT on December 2, 1963 (Figure 8) the spacecraft was close to apogee. At this time there was an apparent sudden increase in ion flux in the 1700-volt channel by about an order of magnitude. This rapid flux increase was followed in approximately three minutes by a sudden impulse type magnetic storm as observed by worldwide ground magnetometer stations. The data obtained during the complete third orbit, Figures 9 and 10, reveal the higher solar wind velocity which persisted in interplanetary space subsequent to the storm commencement on December 2, 1963. This is indicated by the ion current in the higher energy channels. Figure 9 shows that a peak velocity of over 700 km/sec (2790-volt channel) was reached between 1100 and 2100 UT on December 5, 1963. The detailed discussion of this storm and its probable recurrence approximately 30 days later is reserved for a forthcoming report.

Figs.
9 & 10

The majority of the data revealed that in interplanetary space, i.e., beyond the transition region, there were fluctuations in the apparent ion flux from one measurement to the next which sometimes were as large as a factor of 5. This is illustrated by the data obtained for the second outbound pass shown in Figure 8 and again for the latter part of the third orbit (28 to 16 earth radii) shown in Figure 10. During more disturbed times, i.e., at times of high solar wind velocity, the apparent flux tended to fluctuate by more than an order of magnitude. This is clearly illustrated in

the third outbound pass shown in Figure 9. However, at the times of high flux for several hours following the initial impulse at 2113 UT on December 2 (data not shown), the fluctuations were generally much less than an order of magnitude.

It seems highly improbable that these fluctuations were due to variations in total density of the solar wind. This is partially supported by the fact that when interplanetary plasma was observed simultaneously in more than one energy channel, these fluctuations were generally incoherent. In addition, the idea of continuous large magnitude oscillations in plasma density is unappealing due to the profound effect such a phenomena would have on the geomagnetic field and which would most certainly be observable with ground magnetometers. It is also unlikely that these fluctuations were due to sudden changes in the angle of incidence of the solar wind. This latter possibility is ruled out by the fact that the plasma probe had a large angular acceptance in the spacecraft polar plane and that the instrument was a peak reading device on a spinning vehicle. Although there may have been some contribution to these fluctuations from actual intensity changes in the incident flux, it is most likely that the major contribution was from relatively small changes in the solar wind velocity and/or temperature. Because of the high resolution in energy/unit charge of the instrument, only minor changes of velocity would have been required to produce rather large changes in the apparent flux. For example, a deviation of only 2 to 3% in energy from the nominal for a 600-ev monoenergetic proton beam would have decreased the output in the 600-volt channel by a factor of 5.

Since, however, the solar wind was most certainly not monoenergetic, the actual energy shift required to produce these fluctuations would have had to be larger than the above percentages. During periods of high flux associated with the initial phase of disturbances, the energy spectrum of the incident interplanetary solar wind would probably have been much more broad because of the higher temperature of the plasma. This would have prevented the observation of minor shifts in velocity with this instrument. This probably accounts for the smoother appearance of the ion current observed during some of the more disturbed periods in the life of the IMP-I spacecraft at times of high solar wind flux.

2. The Transition Region

For the purposes of this paper the transition region is defined as that volume of space bounded by the outer limit of the earth's magnetosphere on one hand and interplanetary space on the other. It is cautioned, however, that the above definition is by no means exact since the positions of the bounding surfaces are themselves often inexact. The boundary of the magnetosphere (commonly referred to as the magnetopause) is taken to be that surface which confines the well-ordered geomagnetic field [Cahill and Amazeen, 1963] and, in the sunlit hemisphere near the equatorial plane at least, a fairly well-defined high energy particle trapping region [Frank et al., 1963]. It was below this surface that the NASA/Ames Plasma experiment on IMP-I observed no ion flux within the dynamic range of the instrument.

Of all the satellite passes in which plasma was observed by this detector, the vast majority show a rather sharp cutoff in plasma flux associated with the magnetopause. Several passes, however, were anomalous in that they revealed a gradual rather than sharp decrease in ion flux at the magnetopause and, in a few passes, particularly beyond a sun-earth-probe angle of 90° , indicated a transient behavior for this boundary. The outer boundary of the transition region was more difficult to define because of its frequently diffuse and evanescent appearance.

Of the 33 orbits of IMP-I covered in this paper it is probable that only for the first 21 orbits did the spacecraft penetrate into interplanetary space beyond the transition region. After the twenty-first orbit, the outer boundary of the transition region was beyond apogee. Of the 42 passes through the transition region associated with these 21 orbits, 12 passes showed a rather sharp outer boundary while in 28 passes the boundary was to varying degrees nebulous and in at least two passes almost indeterminate.

In those passes that showed a well-defined transition region, the data revealed extremely chaotic plasma flow characterized by high temperatures (broad energy spectra) and variability in the direction of incidence and flux amplitude. Figures 11, 12, and 13 illustrate three of the more dramatic examples of a fairly well-defined transition region. Figure 11, which shows the results obtained during the seventeenth inbound pass, illustrates the appearance of the transition region during disturbed times. A gradual commencement geomagnetic storm occurred during this pass at approximately

Figs.
11, 12, &
13

0830 UT on January 31, 1964, when the spacecraft was at approximately 24 earth radii. Subsequent to this storm beginning, the plasma was observed in the 1700-volt channel only. When the spacecraft reached 15.7 earth radii, the ion flux was observed to shift suddenly from the single channel at 1700 volts to a very broad energy spectrum associated with the simultaneous appearance of flux in all four channels with large fluctuations in both flux and direction of incidence. This was followed by a sharp cutoff of plasma when the spacecraft reached 11.3 earth radii.

Figure 12, showing the thirteenth inbound pass, illustrates an example of a case where beyond the boundary of the transition region the plasma velocity and temperature were probably such that the resulting energy spectrum fell entirely between the energy windows of the detector. Plasma then appeared in the 600-volt channel at 15.2 earth radii and shortly thereafter in the other three channels. Larger fluctuations in the direction of incidence are clearly seen in Figure 12 following the gradual storm beginning which occurred while the spacecraft was embedded in the transition region. The magnetospheric boundary for this pass was very sharply defined by the plasma cutoff at 8.4 earth radii. We attribute the anomalously low altitude for the magnetopause for this thirteenth inbound pass to contraction of the entire magnetosphere caused by an increased plasma pressure associated with the storm. The fifteenth inbound pass shown in Figure 13 again illustrates the appearance of the transition region during the onset of geomagnetic activity. The daily sum of the three hour K_p indices increased from 8- on January 23, 1964, to 20 on January 24, 1964 [Lincoln, 1964]. The onset of this activity was coincident

with the passage of the spacecraft into the transition region near midnight on January 23. Although the geomagnetic activity was minor, the large variability in flux and angle of incidence of the plasma, as well as an indication of a fairly broad energy spectrum, is evident from the data.

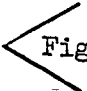
The above three examples of a well-defined transition region are to be contrasted with the less dramatic appearance of the transition region observed during the second outbound, third outbound, and third inbound passes shown in Figures 8, 9, and 10, respectively.

This comparison is particularly noteworthy since over the entire third orbit both the solar wind velocity and the planetary A-index reached higher values than at almost any other period during the three months of observation by IMP-I. The main difference appears to be a lower temperature, less intense flux, and much less variability in flow direction in the transition region during these early orbits as compared to the thirteenth, fifteenth, or seventeenth inbound passes. The transition region data during quiet times, i.e., at times of low solar wind velocity and low A_p , reveal plasma flow characteristics quite similar to those of orbits 2 and 3. During these quiet periods, however, the energy spectra observed in the transition region are shifted to lower energies.

Although the lowest calibrated voltage step corresponded to 600-ev energy acceptance for protons, the instrument was capable of observing lower energy ions within certain limits. Following data sampling at the 600-volt level the high voltage across the analyzer

plates was allowed to decay to zero in order to provide a background check (step 14 in Figure 2). Because of the relatively long time constant of the power supply for this step (approximately one second), there was a small residual voltage across the analyzer plates during the next rotation of the spacecraft. This residual voltage corresponded to a proton energy acceptance which ranged from approximately 25 to 100 ev depending on the direction of arrival of the ions within the sector of azimuthal rotation being examined at the time. Significant ion current in this background channel was frequently observed in the transition region but rarely in interplanetary space. Low energy ions were observed in the transition region, however, only under specific circumstances. They were always present when the free-stream solar wind velocity was low, i.e., when the majority of the interplanetary flux was below the 1700-volt channel. They were also usually observed when the spacecraft was located within the transition region at the time of the onset of geomagnetic disturbances. A significant flux of low energy ions was never observed in the transition region (at times other than the onset of disturbances) when the interplanetary solar wind velocity was high, i.e., above the 1700-volt channel.

Figure 14 shows the average energy spectrum obtained in the transition region during the seventeenth inbound pass (see Figure 11). This spectrum was derived by averaging the current in each energy channel in sector 2 across the entire transition region. The width of the bars represents the full width at half maximum values of energy acceptance for each channel. The lines at approximately 12,000 and


 Fig. 14

13,800 indicate the energy/unit charge acceptance of the two highest channels and shows that no current was observed in these channels. Spectra also obtained for sectors 1 and 3 for this transition region pass showed a shape similar to that in Figure 14 but with greatly reduced intensities. When the differential energy spectrum was derived by dividing the various channel intensities shown in Figure 14 by their appropriate window widths, it became clear that the peak of the spectrum was below the 600-volt channel. Examination of the background channel for this pass reveals no significant current and thus indicates that the peak of the spectrum lay somewhere between 100 and 600 volts, i.e., between 140 and 340 km/sec for protons. Since the entire interplanetary spectrum must have been between 600 and 2970 volts (significant flux only in the 1700-volt channel prior to transition region penetration on the seventeenth inbound pass), this represents a decrease in velocity by a factor of about 2 to 4 as the solar wind passed from a free streaming condition into the transition region. Estimates of the ion temperature in the moving frame of reference of the wind reveal an increase in temperature from less than 10^5 °K in interplanetary space to more than 10^6 °K in the transition region with the development of what appears to be a large nonthermal tail in the ion energy distribution.

In summary, the transition region consistently showed a lower plasma velocity, higher temperature, and greater variability in flow direction compared to the interplanetary solar wind characteristics. In association with the onset of geomagnetic disturbances

these transition region characteristics became even more pronounced, particularly in terms of high temperature and great variability in the direction of flow. It is emphasized that although the ion flow direction was observed to change over large angles, point by point measurements almost always showed that the ion flux was peaked in one of the three azimuthal sectors of rotation. By far the majority of the time sector 2 was the peak flux sector. This indicates that the ion flow direction in the spacecraft equatorial plane usually was contained within the angular limits shown in Figure 6 for the sector containing the probe-sun line. This result is significant in that it appears to be a direct contradiction to the nearly isotropic ion flux in the transition region [Bridge et al., 1964] observed by the MIT plasma probe on this same IMP-I spacecraft. The reason for the apparent disagreement between these two instruments, presumably measuring the same parameters, is as yet unknown.

IV. DISCUSSION OF RESULTS

As was the case with the presentation of the data, the discussion of the results is divided into two sections. The first deals briefly with the observations in interplanetary space. This is followed by a more extensive discussion of the observations in the transition region.

1. Discussion of Interplanetary Observations

The results of the interplanetary measurements generally confirm the findings of earlier measurements, especially those of Neugebauer and Snyder [1962] regarding the parameters that characterize the

solar wind. Estimates of density values for the ionic component of the solar wind derived from this experiment rarely exceeded 1 to 3 ions cm^{-3} except in association with geomagnetic disturbances. Quiet time velocities generally ranged from less than 300 to less than 570 km/sec with a velocity increase to 560 to 750 km/sec during geomagnetically disturbed times.

The somewhat coarse quantization of the velocity data in this experiment was required by the limited telemetry and did not allow a concise representation of the velocity spectrum. On the other hand, since the spacecraft executed a spinning motion, scanning over the celestial sphere took place and we are able to discuss the question of large changes in direction of the incident flux. In this regard it is clear that at no time was a significant flux observed outside of sector 2 (the sector containing the solar direction) when the spacecraft was in the free interplanetary stream. This result is in complete agreement with the somewhat limited observations of the Explorer 14 plasma probe [Wolfe and Silva, 1964] which showed the interplanetary plasma to be incident always from the solar direction within the 18° quantization of the Explorer 14 telemetry system.

Evidently the narrow energy windows, separated by gaps, were responsible for the nonobservation of the solar wind flux for about 30% of the time. Thus, when the velocity distribution function was narrow and the mean velocity of the stream centered between two energy windows, apparent disappearance of the solar wind flux was likely. This conclusion is supported by the fact that ion current was always observed during the initial phase of a geomagnetic storm when the velocity spectrum broadened.

It has been previously stated that the individual velocity measurements obtained with the IMP-I plasma probe were somewhat coarse as a result of the quantization of the analyzer voltage. This quantization uncertainty may be expected to become statistically insignificant, however, if the velocity is averaged over a sufficiently long period. In this regard consider the average interplanetary solar wind velocity obtained during the first 21 orbits of IMP-I (November 27, 1963 to February 15, 1964). This velocity was determined to be 378 km/sec and it represents a time weighted average which took into account only that portion of the time the IMP-I satellite was actually in interplanetary space. It is interesting to consider some of the implications of this average velocity. It has long been theorized [Parker, 1958] that the consequences of solar rotation and the efflux of ionized solar gas from a nonfield free region of the solar atmosphere would produce an interplanetary magnetic field structure resembling an Archimedean spiral. The resulting spiral angle of the interplanetary magnetic field would then be a function of the angular velocity of the solar atmosphere, the solar wind velocity, and the distance from the sun at which the spiral angle is being considered. The expected spiral angle at the orbit of earth for a 378 km/sec solar wind velocity would be approximately 47° . This is the 'average' acute angle that the interplanetary field lines, regardless of polarity, would be expected to make with the earth-sun line in the ecliptic plane as measured clockwise when viewed from the north ecliptic pole. Note that the above spiral angle was calculated assuming photospheric detachment

of the ejected solar gas. Corotation of the corona to several solar radii, however, would not appreciably alter the expected spiral angle.

The 47° spiral angle, calculated from consideration of the solar wind alone, is evidently about midvalued between the 30° to 70° limits for the most preferred spiral angle of the interplanetary magnetic field (regardless of polarity) observed by the IMP-I magnetometer over this same time period [Ness and Wilcox, 1965]. It is cautioned that the above correlation of average quantities is somewhat nebulous and comparisons of solar wind velocities and magnetic field orientations over a shorter time period (preferably during nondisturbed conditions) are necessary in order to provide information on the detailed correspondence of the spiral angle and the streaming velocity.

Perhaps a more meaningful consequence of a 378 km/sec average solar wind velocity is that it represents an average sun-earth propagation time of 4.7 days. Over approximately the same 2-1/2 month time period, Ness and Wilcox [1965] performed a time cross-correlation between the interplanetary magnetic field orientation observed on IMP-I and the solar photospheric field orientation obtained from magnetographs taken at Mt. Wilson. Their findings show a strong correspondence for a 4.5 ± 0.5 day lag from the central meridian passage of a given photospheric field configuration to a corresponding interplanetary field configuration observed on IMP-I. This lag is quite consistent with the propagation time determined from the average solar wind velocity and evidently lends substantial support to the interplanetary solar wind and magnetic field model proposed by Parker [1958].

It seems apparent from the interplanetary data that rapid (period less than 5 minutes) small-amplitude fluctuations were always present in the velocity of the solar wind even during geomagnetically quiet periods. These fluctuations increased in amplitude, however, during geomagnetic storms. The frequency of these fluctuations were apparently more rapid than the 5-minute complete cycle time of the plasma probe. The cause of these velocity fluctuations is not completely clear but they may be associated, in part, with small scale variations of temperature in the solar corona. It is likely, however, that this coronal fine structure is appreciably altered in propagating over a distance of 1 AU. The consequences of these velocity fluctuations are also unclear at this time; however, they undoubtedly have a profound effect on the characteristics of the transition region. More specifically, they would have great bearing on any discussion concerning the formation and stability of a collisionless magnetohydrodynamic bow shock presumably associated with the outer boundary of the transition region (see next section).


The interplanetary data and the discussion presented thus far are meant to provide the input information for the transition region and thereby give a basis for its discussion. A detailed study of the geophysical response to the dynamic character of the interplanetary solar wind will be discussed in another report.

2. Discussion of Transition Region Observations

Although the first traversal of the magnetopause was evidently made with the search coil experiment on the Pioneer I space probe [Sonett et al., 1960b; Sonett et al., 1960a], command interruptions of the telemetry signals precluded observation of the magnetopause itself, and only the regular fields of the magnetosphere and the turbulent fields of the transition region were observed. The first recurrent detection of the boundary was obtained with the Explorer 12 magnetometer experiment reported by Cahill and Amazeen [1963]. A more detailed map of the magnetic boundary of the magnetosphere was acquired with the IMP-I magnetometer [Ness et al., 1964]. From the standpoint of the solar wind and its relation to the magnetopause, clarification was begun with the plasma observations on Explorer 10 [Bonetti et al., 1963] and Explorer 14 [Wolfe and Silva, 1964]. Today the region of trapping for superthermal and high energy particles is known from the extensive mapping carried out by Frank et al., [1963] with a variety of detectors on Explorers 12 and 14. Within this space, the regular magnetosphere, we have found no detectable flux of low energy ions. From this we are able to deduce that the omnidirectional flux in the instrumental energy range must have been below the values from $7.2 \times 10^4 \text{ cm}^{-2} \text{ sec}^{-1} \text{ ev}^{-1}$ for 600-ev protons to $1.1 \times 10^4 \text{ cm}^{-2} \text{ sec}^{-1}$ for 4000-ev protons.

One of the major results from the IMP-I satellite has been the mapping of the extent of the transition region and its outer limits. This mapping has resulted from observations made by several of the

instruments aboard the spacecraft and the results have sometimes led to different inferences, this experiment being no exception. We have, in view of some of the differing definitions of the transition region which are now in vogue, taken as our criteria the breadth of the ion energy spectrum and the variations in the angle of incidence of the flux. The extent of the transition region has been mapped in terms of the contrast between these quantities when observed in different regions of space. For example, the lack of measurable flux in the magnetosphere defined its extent. The outer boundary was often considerably more difficult to assess, as a distinct transition was not always evident according to the criterion of a sudden change in plasma entropy. Using the stated criteria, however, we have plotted in Figure 15 the extent of the transition region for each of the orbital passes. The extremities of the solid lines represent the positions of the boundaries that confine the transition region. The dashed lines show the boundary limits for those passes in which the termination of the transition region was uncertain. This plot was derived by locating the transition region in terms of geocentric distance and solar oriented ecliptic longitude. It therefore does not account for the latitude of the spacecraft during its traversal through this region. Superimposed on the data is the theoretical gasdynamic standing shock wave expected to form for the high Mach number flow of the solar wind and associated blunt body shape of the magnetosphere. These theoretical curves are taken from the work of Spreiter and Jones [1963] and are calculated for a solar wind velocity of 600 km/sec, a density of $2.5 \text{ protons cm}^{-3}$, a tangential magnetic field of 5 gamma, and an Alfvén Mach number of 8.71. Two shock waves


 Fig. 15

are shown corresponding to two possible values for the ratio of specific heats, γ , of the incident gas. Note from Figure 15 that the boundary of the magnetosphere flares out from the subsolar point and ultimately becomes approximately parallel to the earth-sun line. The mean standoff distance of the outer boundary of the transition region from the magnetopause appears to be 4 to 5 earth radii at the subsolar point and increases with increasing angle from the subsolar point.

The later orbits in Figure 15 reveal a systematic difference in magnetopause locations between outbound and inbound passes. This is perhaps suggestive of the curvature of the magnetosphere about the earth-sun line. In order to investigate the possibility of an asymmetry in the gross structure of the magnetosphere, the transition region boundary crossings (and the connecting points along the orbits) were rotated into the ecliptic about their respective points of projection on the earth-sun line. The results of this rotation are seen in Figure 16. Inspection of this figure shows the somewhat closer agreement in successive magnetopause traversals suggesting cylindrical symmetry of the magnetosphere about the earth-sun line, at least at angles not too large from the ecliptic. Any closer agreement is not necessarily to be expected because of transient nature of the boundary as was observed particularly in the later orbits where the spacecraft was on the night side of the earth. Any further correction to the positions of the boundaries seems unwarranted in view of this transient behavior. Tables 1 and 2 list the locations of the magnetopause and the outer boundary of the

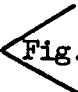



Fig. 16



Tables
1 & 2

transition region observed by the plasma probe on IMP-I through the first 30 orbits. The locations are given in terms of geocentric distance in earth radii, universal time, and geographic coordinates.

The locations of the transition region as defined by our results have been compared on corresponding orbital passes to the observations of energetic electrons ($E > 45$ kev) on IMP-I as reported by Anderson et al. [1965]. All of the early inbound passes reported (passes nearest the subsolar point) show good correlation between the plasma flow cutoff and the beginning of a well-defined trapping region. Sporadic electron fluxes substantially above the interplanetary background (but well below the levels of the outer radiation zone) were also reported [Anderson et al., 1965] at locations both in and beyond the transition region deduced from the plasma data. The above seemed true irrespective of the sun-earth-probe angle; however, energetic electrons in and beyond the transition region appear much more profuse at larger angles from the subsolar point. These sporadic fluxes were interpreted by Anderson et al. [1965] as trapped electrons which had been 'sloughed off' the magnetosphere. Their principal argument for this seemed to be the consistent observation of a decreased amplitude of the isolated electron peaks with increasing distance upstream from the magnetopause.

Scarf et al. [1965] proposed that the expected high electron to ion temperature ratio would cause the transition region to become unstable with respect to the production of ion acoustic waves. They further suggest that the resulting electric field oscillations could

accelerate solar wind electrons to high energies by means of the cyclotron resonance. In view of the high degree of turbulence of the ion component of the plasma in the transition region which we have observed on IMP-I, the above seems to be a plausible alternate to the suggestions of Anderson et al. [1965] regarding these electron fluxes. As suggested by Scarf et al. [1965], the higher amplitude electron peaks observed near the magnetospheric boundary might simply represent the most probable region of ion wave dissipation.

It is interesting to note that the results of Anderson et al. [1965] show that for the second inbound pass of IMP-I, which was subsequent to the large disturbance of December 2, 1963, the transition region was copiously filled with energetic electrons. This is contrasted to the observations two orbits later during the fourth inbound pass which revealed not only the lack of anomalous electron fluxes in the transition region but also an appreciable depletion of the outer radiation zone. Anderson et al. [1965] attributed the appearance of their data on the fourth inbound pass to a weakened magnetospheric source which could not supply observable fluxes of electrons to the transition region. In comparison, the plasma data showed that during the fourth inbound pass of IMP-I there was no observable ion flux above 600 ev/unit charge in either interplanetary space or in the transition region. The only evidence of a transition region during the fourth inbound pass was a moderate flux of ions within the 25-to 100-volt range observed in the background channel. It is therefore alternatively suggested that because of the weak

character of the solar wind as evidenced by its very low velocity, there was insufficient electron acceleration in the transition region to produce observable high energy electron fluxes. It is further suggested that solar wind electrons, accelerated in the transition region and subsequently injected into the magnetosphere, are a principal source for the outer radiation zone. Thus the depleted character of the outer zone observed by Anderson et al. [1965] on the fourth inbound pass of IMP-I might simply be the result of the outer zone loss rate being greater than the injection rate from the transient region at that time.

Although charged particle injection might occur anywhere along the magnetopause, it is conceivable that it could occur more readily along the tail of the magnetosphere where the magnetic field is expected to be weak. Two observations by the plasma probe support this possibility. The first pertinent observation was the frequently transient behavior of the magnetopause at large sun-earth-probe angles, particularly at angles greater than 90° . The apparent rapid motion of the magnetosphere boundary at these large angles was also observed by Bonetti et al. [1963] on Explorer 10. The second is concerned with the observation of a highly turbulent transition region on some of the very last passes of IMP-I out of the magnetosphere at sun-earth-probe angles exceeding 120° . It is proposed that the high plasma temperature and magnetopause instability suggested by the above observations, combined with the expected weak magnetic field, might allow the injection of charged particles along the tail of the

magnetosphere to take place more easily than at the nose where the field would be stronger and where the boundary has been observed to be fairly stable.

The location of isolated peaks of electrons with $E > 30$ kev observed by Fan et al. [1964] on IMP-I were also compared to our observations. These peaks of energetic electrons were reported as possibly being accounted for by the acceleration of lower energy electrons by the collisionless magnetohydrodynamic standing shock which presumably defines the outer boundary of the transition region. From this data Fan et al. [1964] located the wave front by the position of the electron peak farthest upstream. The shock position defined in this way does not seem to correlate well with the outer boundary of the transition region as determined by the plasma data. Out of 32 passes reported by Fan et al. [1964] only 7 show the outermost peak of electrons to coincide within 0.5 earth radius to the outer boundary of the transition region as defined by our previously stated criteria. In some cases these electron spikes are reported far upstream from this boundary. It seems more plausible that these energetic electrons may be the result of local acceleration processes which owe their origin to the turbulence in the transition region itself, as discussed previously.

The initial results of the IMP-I magnetometer experiment, as reported by Ness et al. [1964], consistently revealed a region of magnetic turbulence between the termination of the earth's regular magnetic field and the relatively smooth fields encountered in interplanetary space. The outer boundary of this region of magnetic

turbulence was noted by the rather sharp change in amplitude of the 5.46 minute variances in the components of the ambient magnetic field and was interpreted by Ness et al. [1964] as evidence for a collisionless magnetohydrodynamic shock wave.

Comparison of available data showed that within 0.5 earth radius the outer boundary of the transition region, as determined by the plasma data, corresponded in location to the outer boundary of magnetic turbulence [Ness et al., 1964] for approximately 79% of the passes of IMP-I. The magnetopause positions, reported by Ness et al. [1964] from the IMP-I magnetic field experiment, were compared to the point at which plasma flow stopped on each pass of the satellite and were found to agree within 0.5 earth radius 64% of the time. Careful scrutiny of the plasma data for those passes where there was disagreement between our observations and those of the magnetometer showed that, with the exception of a few anomalous cases, the majority of these passes exhibited a diffuse outer boundary to the transition region or a transient character in the location of the magnetopause. Although the present agreement seems fairly good, it is suggested that the uncertainty in the application of the criteria used to define the boundaries as observed by the various experiments will, upon precise comparison and analysis, prove to be the cause of the majority of the present discrepancies.

In addition to the curved plate analyzer, the IMP-I satellite also carried a Faraday cup type plasma detector in its experiment repertoire. This experiment was conducted by the Massachusetts Institute of Technology and the preliminary results were reported

by Bridge et al. [1964]. Our results agree in general with the MIT results in most of the gross features of the data; however, there are apparently significant differences in some of the finer details of the plasma characteristics. For example, the extent and location of the transition region as determined by these two plasma detectors seem to be in fairly good correspondence. Our data do not show, however, the hot isotropic flux of ions in the transition region which Bridge et al. [1964] reported. Inspection of the transition region data in Figures 8 through 13 shows that although the ion flow direction tended to exhibit great variability, it is clear that the majority of the flux was contained within the angular extent defined by sector 2 (see Figure 6). An omnidirectional flux of the magnitude reported by Bridge et al. [1964] would have resulted in our observation of approximately equal ion currents in all three angular sectors. This was clearly not observed. In addition, the MIT plasma probe apparently has consistently measured a lower solar wind velocity than has been observed by the curved plate analyzer. The average interplanetary solar wind velocity as determined by the MIT Faraday cup during the first 2-1/2 months of satellite life was 319 km/sec [Ness and Wilcox, 1965]. This is to be compared with the average velocity of 378 km/sec determined by the Ames plasma probe over the same time period. The MIT data also show [Bridge et al., 1964] a rather significant and apparently directed ion flux observed within the magnetosphere. This also was not observed by the curved plate detector.

Although the two instruments functioned quite differently, their operational differences evidently cannot account for the observed discrepancies in the results. Investigations conducted to date have not uncovered any clear explanation for the apparent observational differences between these two plasma probes. In support, however, of the results of the Ames plasma experiment on IMP-I, it is clear that there was good agreement with the previous results of curved plate plasma probes on both Explorer 14 [Wolfe and Silva, 1964] and Mariner 2 [Neugebauer and Snyder, 1962]. In addition, there seems to have been excellent correspondence with the magnetic field spiral angle and central meridian lag of photospheric field configurations determined by Ness and Wilcox [1965] from IMP-I magnetometer data.

It is apparent that the mean shape of the outer boundary of the transition region very closely resembles the calculated shock front. The very sudden disorder of the plasma ions on many passes, such as the thirteenth, fifteenth, and seventeenth, strongly suggests what one might expect for a high Mach number shock. There are, however, many details of the data which need to be explained. For example, a simple shock theory does not account for the rather diffuse character of the outer boundary for more than half of the passes and the frequent appearance of energetic electrons [Fan et al., 1964; Anderson et al., 1965] upstream from the outer boundary of the transition region. Although these features do not rule out the existence, at least part of the time, of a magnetohydrodynamic shock wave, great care must be utilized in attempting any simple extrapolation of collision dominated gas kinetic shock theory. It seems clear, in

any instance, that the high velocity flow of solar wind must be deflected around the magnetosphere in some complicated manner and, indeed, this is indicated by all the available evidence as well as common sense. Such a plasma deflection, in order to satisfy the criteria of a shock wave, must generate entropy. It is plausible to think of some means of destroying order other than a simple collisional process which must be ruled out in this instance. More exotic processes might include the generation of electromagnetic and hydromagnetic radiation. The kind of data presently available seems to point to some such process. What is most remarkable is that the relatively simple Rankine-Hugoniot equations, together with a rudimentary equation of state, should satisfy the problem of a collisionless magnetohydrodynamic shock as well as seems to be the case [Sonett et al., 1964]. This is especially surprising in view of the differing equations of state that probably apply to the flow on the upstream and downstream sides of the shock wave and the unsteady character of the solar wind itself. Lastly, since several modes of propagation are available in an anisotropic medium, such as the magnetoionic one being considered here, both the mode of propagation and the appropriate Mach number must be considered. Since the slow mode requires that the field and gas have pressure jumps in opposite senses and since the Alfvén mode is incompressible [Anderson, 1963], it appears correct to utilize the fast mode group velocity. Then for the flow to be supersonic it is simply necessary for the local propagation velocity to be exceeded by the flow velocity. Since this depends upon direction with respect to the local magnetic

field, it might be expected that the local Mach number for the flow will vary depending upon location over the shock face. This conclusion is in agreement with the magnetohydrodynamic generalization of the Rankine-Hugoniot equations found for the October 7, 1962, event [Sonett et al., 1964] where the fast mode shock was a necessary condition for a post shock Mach number < 1 .

Although it is somewhat difficult to support the view of Fan, et al. [1964] regarding the shock aspects of their electron pulses, there are many features of our data which support the applicability of the suggestions of Axford [1962] and of Kellogg [1962] and the aerodynamic calculations of Spreiter and Jones [1963] which all predict the formation of a bow shock upstream from the magnetopause. In contrast to the above, there are many features of the IMP-I data that support the picture of a broad disordered region between the earth's field and the interplanetary medium as proposed by Bernstein et al. [1964] and discussed more recently by Scarf et al. [1965], which evidently precludes the formation of a shock front.

In light of our IMP-I results and other presently available data, it seems pragmatic to suppose that the solar wind with its embedded magnetic field may be only marginally capable of producing a detached shock wave. If this is so, then it appears reasonable that a shock wave may form only under the special conditions of higher flux and velocity present during more disturbed periods.

In any event, all available data point to the extreme complexity of a transition region dominated by phenomena such as local acceleration, injection and diffusion of high energy electrons, twisted magnetic

fields, turbulent plasma flow, and probably a great variety of wave phenomena. Perhaps even of more importance is the apparent ease with which minor solar activity can evidently alter drastically the characteristics of this region. It seems clear that a great many detailed measurements of transition region phenomena will be required in order to shed light on its true nature.

ACKNOWLEDGEMENTS

The authors wish to thank M. Bader, R. C. Hedlund, and the personnel of the Instrumentation Division at Ames Research Center for their role in the design, fabrication, and integration of the NASA/Ames plasma probe for the IMP-I spacecraft. We are indebted to H. Tashjian for his assistance in preparing the machine program for the reduction of the data. We are grateful to the Goddard Space Flight Center personnel responsible for the success of the IMP-I mission. We would finally like to thank C. P. Sonett and J. R. Spreiter for many helpful and stimulating discussions concerning the data.

REFERENCES

- Anderson, J. E., Magnetohydrodynamic shock waves, M. I. T. Press, Cambridge, Massachusetts, 1963.
- Anderson, K. A., H. K. Harris, and R. J. Paoli, Energetic electron fluxes in and beyond the earth's outer magnetosphere, J. Geophys. Res., 70, 1039-1050, 1965.
- Axford, W. I., The interaction between the solar wind and the earth's magnetosphere, J. Geophys. Res., 67, 3791-3796, 1962.
- Bernstein, W., R. W. Fredricks, and F. L. Scarf, A model for a broad disordered transition between the solar wind and the magnetosphere, J. Geophys. Res., 69, 1201-1210, 1964.
- Bonetti, A., H. S. Bridge, A. J. Lazarus, B. Rossi, and F. Scherb, Explorer 10 plasma measurements, J. Geophys. Res., 68, 4017-4063, 1963.
- Bridge, J., A. Egidi, A. Lazarus, E. Lyon, and L. Jacobson, Preliminary results of plasma measurements on IMP-A, COSPAR Preprint, Florence, Italy, May 1964.
- Cahill, L. J., and P. G. Amazeen, The boundary of the geomagnetic field, J. Geophys. Res., 68, 1835-1843, 1963.
- Coleman, P. J., Jr., Characteristics of the region of interaction between the interplanetary plasma and the geomagnetic field: Pioneer 5, J. Geophys. Res., 69, 3051-3076, 1964.
- Fan, C. Y., G. Gloeckler, and J. A. Simpson, Evidence for > 30 - keV electrons accelerated in the shock transition region beyond the earth's magnetospheric boundary, Phys. Rev. Letters, 13, 149-152, 1964.
- Frank, L. A., J. A. Van Allen, and E. Macagno, Charged-particle observations in the earth's outer magnetosphere, J. Geophys. Res., 68, 3543-3554, 1963.

- Gringauz, K. I., Investigation of interplanetary plasma and planetary ionospheres by means of charged particle traps on space rockets, XIIth International Astronautical Congress, Washington, D. C., October 4, 1961.
- Heppner, J. P., N. F. Ness, C. S. Scarce, and T. L. Skillman, Explorer 10 magnetic field measurements, J. Geophys. Res., 68, 1-46, 1963.
- Kellogg, P. J., Flow of plasma around the earth, J. Geophys. Res., 67, 3805-3811, 1962.
- Lincoln, J. V., Geomagnetic and solar data, J. Geophys. Res., 69, 2380, 1964.
- Ness, N. F., C. S. Scarce, and J. B. Seek, Initial results of the IMP-I magnetic field experiment, J. Geophys. Res., 69, 3531-3569, 1964.
- Ness, N. F., and J. M. Wilcox, Extension of the photospheric magnetic field into interplanetary space, Goddard Space Flight Center report X-612-65-79, Feb. 1965.
- Neugebauer, M., and C. W. Snyder, Preliminary results from Mariner 2 solar plasma experiment, Jet Propulsion Laboratory Technical Memorandum 33-111, November 15, 1962.
- Parker, E. N., Dynamics of the interplanetary gas and magnetic fields, Ap. J., 128, 664-676, 1958.
- Parker, E., Extension of the solar corona into interplanetary space, J. Geophys. Res., 64, 1675-1681, 1959.
- Scarf, F. L., W. Bernstein, and R. W. Fredricks, Electron acceleration and plasma instabilities in the transition region, J. Geophys. Res., 70, 9-20, 1965.

- Sonett, C. P., Magnetic compression in the geomagnetic field as measured by Pioneer I, Proc. Astro. Soc. (Pacific), 71, 390-392, 1959.
- Sonett, C. P., D. S. Colburn, L. Davis, Jr., E. J. Smith, and P. J. Coleman, Jr., Evidence for a collision-free magnetohydrodynamic shock in interplanetary space, Phys. Rev. Letters, 13, 153-156, 1964.
- Sonett, C. P., D. L. Judge, A. R. Sims, and J. M. Kelso, A radial rocket survey of the distant geomagnetic field, J. Geophys. Res., 65, 55-68, 1960a.
- Sonett, C. P., E. J. Smith, and A. R. Sims, Surveys of the distant geomagnetic field: Pioneer I and Explorer XI, in Space Research, pp. 921-937, edited by H. J. Kallmann-Bijl, North Holland Publishing Co., Amsterdam, 1960b.
- Spreiter, J. R., and W. P. Jones, On the effect of a weak interplanetary magnetic field on the interaction between the solar wind and the geomagnetic field, J. Geophys. Res., 68, 3555-3564, 1963.
- Wolfe, J. H., and R. W. Silva, Observation of the October 7, 1962, magnetic disturbance in space, 2: Explorer 14 plasma probe, Trans. Amer. Geophys. Union, 45, 79, 1964.

TABLE 1. The magnetopause location and the position of the outer boundary of the transition region for the first thirty outbound passes in earth radii, universal time (day-hour), and geographic coordinates.

Outbound Passes								
Orbit	Magnetopause Boundary				Outer Termination of Transition Region			
	Geocentric Distance (R_E)	Time	Lat.	Long.	Geocentric Distance (R_E)	Time	Lat.	Long.
1	12.2	331-0825	-31.9	-4.1	16.9-	331-1230	-30.3	-57.5
					17.1	331-1245	-30.2	-60.9
2	10.9	335-0455	-32.3	41.6	15.1-	335-0815	-30.8	-0.1
					16.1	335-0910	-30.5	-12.4
3	10.9	339-0215	-32.0	77.5	13.6-	339-0415	-31.1	53.1
					14.0	339-0435	-31.0	48.8
4	11.3	342-2335	-31.9	114.4	16.4	343-0350	-30.2	60.1
5	12.0	346-2135	-32.0	142.8	15.0	347-0000	-31.0	112.1
6	10.7	350-1815	-32.2	-174.5	18.6	351-0105	-29.5	96.6
7	11.7	354-1550	-31.8	-140.7	16.7	354-2010	-30.1	163.7
8	13.0	358-1405	-31.4	-115.1	17.7	358-1820	-29.8	-171.1
9	11.9	362-1035	-31.7	-68.9	17.0-	362-1500	-29.9	-125.9
					17.4	362-1525	-29.8	-131.6
10	13.1	001-0845	-31.1	-43.0	18.8-	001-1410	-29.2	-115.0
					20.5	001-1615	-28.6	-144.1
11	14.4	005-0650	-30.6	-15.8	18.8-	005-1115	-29.1	-75.1
					24.5	005-1910	-27.1	173.0
12	12.3	009-0230	-31.7	41.7	13.8-	009-0340	-31.1	27.2
					17.4	009-0700	-29.8	-16.9
13	16.1-	013-0310	-30.1	34.3	20.5-	013-0800	-28.6	-32.0
	17.7	013-0445	-29.6	13.0	20.8	013-0825	-28.5	-37.8

TABLE 1. (Concluded)

Outbound Passes								
Orbit	Magnetopause Boundary				Outer Termination of Transition Region			
	Geocentric Distance (R_E)	Time	Lat.	Long.	Geocentric Distance (R_E)	Time	Lat.	Long.
14	14.7	016-2255	-30.5	91.6	19.0-	017-0315	-29.0	33.3
					21.3	017-0610	-28.2	-7.4
15	16.3-	020-2130	-30.0	111.9	22.8	021-0525	-27.7	2.0
	16.7	020-2155	-29.8	106.3				
16	15.8-	024-1820	-30.2	154.9	22.2-	025-0150	-27.8	51.3
	16.5	024-1900	-29.9	146.0	23.9	025-0425	-27.2	14.5
17	15.5	028-1515	-30.1	-163.5	22.8-	028-2355	-27.5	76.7
					25.7	029-0455	-26.4	5.2
18	14.9-	032-1140	-30.3	-114.8	25.3-	033-0105	-26.5	58.3
	17.6	032-1420	-29.4	-150.3	26.9	033-0425	-25.9	10.2
19	17.7	036-1140	-29.6	-113.5	26.7-	037-0115	26.0	54.0
					28.1	037-0435	-25.3	5.7
20	19.7	040-1125	-28.7	-111.1	26.4	040-2200	-26.0	98.4
21	18.7	044-0715	-29.1	-53.9	30.3	045-0645	-23.7	-31.3
22	19.5	048-0515	-28.9	-26.4	31.3-	049-1050	-22.5	-93.6
					31.5	049-1450	-21.7	-152.2
23	20.6	052-0355	-28.4	-8.6	> 31.5			
24	21.7	056-0240	-27.9	7.7	"			
25	25.9	060-0620	-26.2	-46.3	"			
26	22.6-	063-2210	-27.7	69.1	"			
	23.9	064-0015	-27.1	39.4	"			
27	≤ 30.7	068-1620	-23.0	163.4	"			
28	26.7	072-0010	-25.7	36.2	"			
29	30.7	076-1020	-22.9	-114.3	"			
30	30.2	080-0510	-23.3	-41.4	"			

TABLE 2. The magnetopause location and the position of the outer boundary of the transition region for the first thirty inbound passes in earth radii, universal time (day-hour), and geographic coordinates.

Inbound Passes								
Orbit	Magnetopause Boundary				Outer Termination of Transition Region			
	Geocentric Distance (R_e)	Time	Lat.	Long.	Geocentric Distance (R_e)	Time	Lat.	Long.
1	11.1	334-1900	-9.5	-110.3	13.3	334-1720	-11.6	-88.8
2	10.3-	338-1645	-8.4	-78.4	12.1-	338-1530	-10.4	-62.8
	10.4	338-1640	-8.6	-77.4	13.1	338-1445	-11.3	-53.1
3	11.1	342-1320	-9.2	-32.3	14.3-	342-1050	-12.2	0.3
					16.1	342-0915	-13.5	21.9
4	11.0	346-1050	-8.5	1.4	14.8	346-0750	-12.1	40.7
5	12.1	350-0725	-9.3	48.0	15.2-	350-0450	-12.1	82.2
					16.2	350-0355	-12.8	94.7
6	8.3	354-0700	-4.1	58.7	10.9-	354-0520	-7.9	77.8
					12.0	354-0430	-9.2	88.2
7	10.3-	358-0255	-7.0	111.3	14.6-	357-2340	-11.4	153.1
	11.6	358-0200	-8.6	122.5	15.0	357-2315	-11.7	158.7
8	9.2	362-0100	-5.1	139.0	14.4	361-2110	-11.0	-172.7
9	13.3	365-1915	-10.0	-145.8	16.1	365-1645	-12.3	-112.2
10	11.6	004-1735	-8.2	-121.7	16.3	004-1335	-12.4	-68.6
11	9.9	008-1605	-5.6	-100.1	13.9	008-1310	-9.9	-63.2
12	10.6	012-1300	-6.0	-58.0	16.2-	012-0820	-11.6	3.1
					18.1	012-0625	-13.0	29.6
13	8.4	016-1125	-2.6	-32.5	15.2	016-0620	-10.8	30.8
14	12.8	020-0530	-8.5	42.8	16.9	020-0150	-12.0	92.1

Table 2. (Concluded)

Inbound Passes

Orbit	Magnetopause Boundary				Outer Termination of Transition Region			
	Geocentric Distance (R_E)	Time	Lat.	Long.	Geocentric Distance (R_E)	Time	Lat.	Long.
15	9.4	024-0510	-4.1	50.7	16.4	023-2335	-11.4	122.7
16	13.2	027-2335	-8.7	123.6	19.2	027-1745	-13.3	-156.6
17	11.3	031-2205	-6.5	145.7	15.7	031-1825	-10.8	-166.3
18	14.8	035-1635	-9.6	-141.8	19.5-	035-1140	-13.2	-73.7
					23.5	035-0610	-15.6	4.8
19	11.0	039-1655	-5.3	-143.8	22.0	039-0545	-14.5	9.1
20	10.7	034-1410	-4.8	-105.6	20.3-	043-0500	-13.4	18.3
					24.7	042-2225	-16.0	112.5
21	11.2-	047-1055	-5.4	-62.2	23.2	046-2205	-15.1	115.0
	14.6	047-0815	-9.0	-27.6				
22	11.6	051-0755	-5.7	-21.9	30.5-	050-0055	-19.8	60.2
					31.5	049-1450	-21.7	-152.2
23	17.6	054-2350	-11.1	87.2	30.7-	053-2100	-20.0	114.8
					31.5	053-1205	-21.7	-114.6
24	15.4	058-2300	-9.4	98.5	> 31.5			
25	20.4	062-1455	-12.7	-150.3	"			
26	17.0-	066-1610	-9.9	-168.8	"			
	21.3	066-1110	-12.9	-98.3				
27	22.1-	070-0705	-13.4	-41.7	"			
	26.3	069-2350	-16.0	62.9				
28	19.3-	074-0755	-11.4	-55.5	"			
	24.9	073-2350	-15.0	60.3				
29	23.7-	077-2315	-14.1	66.3	"			
	27.1	077-1640	-16.3	161.8				
30	≤ 23.8	081-2020	-14.0	106.3	"			

FIGURE CAPTIONS

- Figure 1. Schematic diagram of the NASA/Ames plasma probe showing the ion optics and electronics.
- Figure 2. Nominal ion acceptance energy per unit charge as a function of step number.
- Figure 3. Configuration of entrance aperture, analyzer plates, and collector showing the disposition with respect to the IMP-I spacecraft equatorial and polar planes.
- Figure 4. Typical ϕ acceptance curve for a beam potential of 600 volts and θ set equal to zero.
- Figure 5. Plasma probe angular acceptance fan and orientation with respect to the IMP-I spacecraft.
- Figure 6. Data acquisition and timing diagram showing the azimuthal sector widths and locations with respect to the spacecraft-sun line.
- Figure 7. IMP-I equatorial plane and noon meridian plane orbit projections and positions of apogee for the first seventeen orbits.
- Figure 8. Data obtained during the second outbound pass of the IMP-I satellite showing the observed incident ion current in the three azimuthal sectors for the four lowest energy steps as a function of universal time and geocentric distance in earth radii.
- Figure 9. Data for the third outbound orbit.
- Figure 10. Data for the third inbound orbit.

- Figure 11. Data for the seventeenth inbound pass showing the outer boundary of the transition region at 15.7 earth radii and the magnetopause at 11.3 earth radii.
- Figure 12. Data for the thirteenth inbound pass showing the outer boundary of the transition region at 15.2 earth radii and the magnetopause at 8.4 earth radii.
- Figure 13. Data for the fifteenth inbound pass showing the outer boundary of the transition region at 16.4 earth radii and the magnetopause at 9.4 earth radii.
- Figure 14. The average energy spectrum over the entire transition region during the seventeenth inbound pass. The data was obtained in sector 2 (solar sector) with the energy window widths depicted by the width of the bars.
- Figure 15. Transition region traversals shown in the IMP-I orbit plane with two shock locations for $\gamma = 2$ and $\gamma = 5/3$ and magnetopause location for a plasma velocity of 600 km/sec, density 2.5 protons/cm³, magnetic field 5γ , and Alfvén Mach number of 8.7.
- Figure 16. Transition region traversals rotated into the ecliptic about their projections on the earth-sun line.

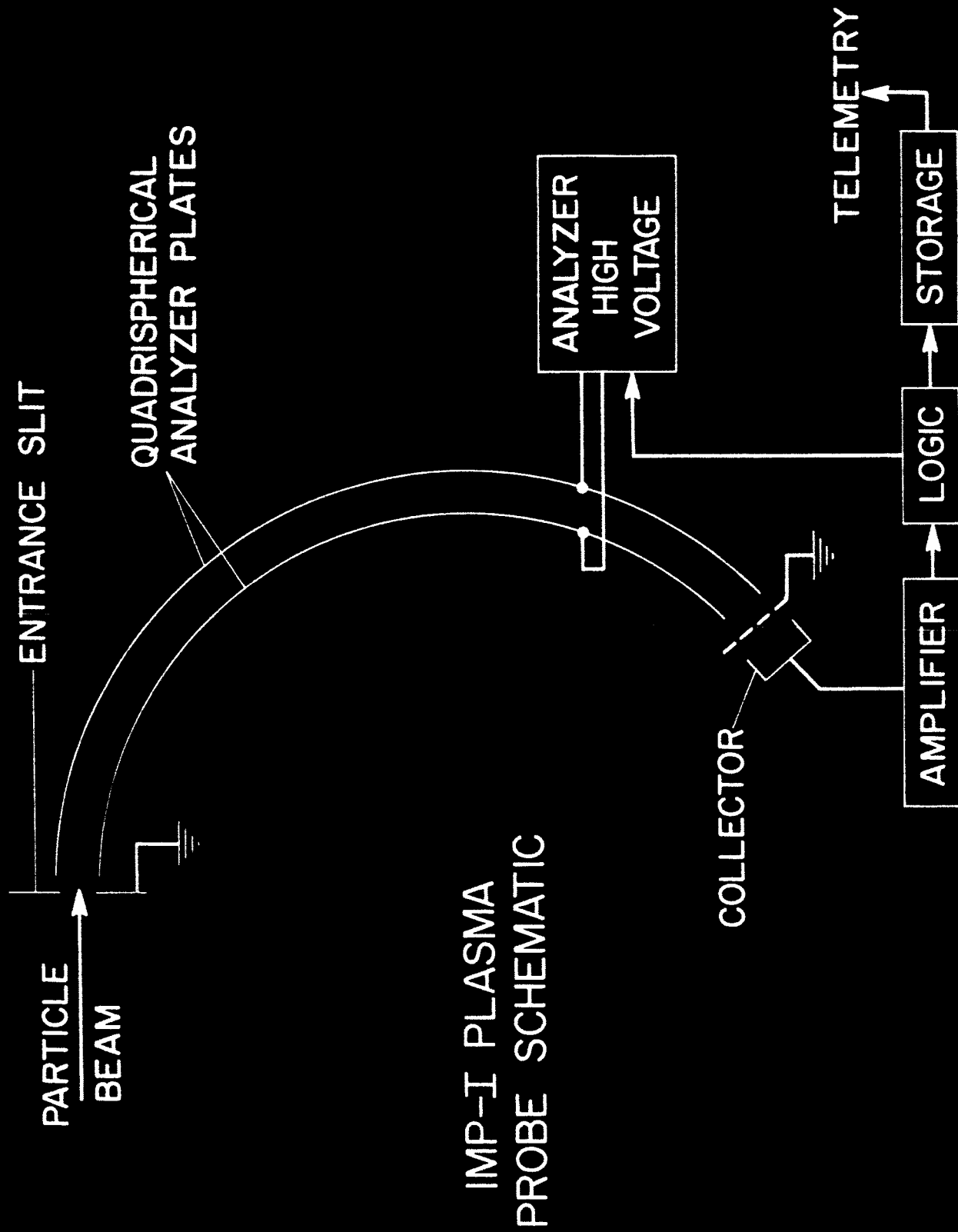


Figure 1.

IMP-I PLASMA PROBE ENERGY STEPS

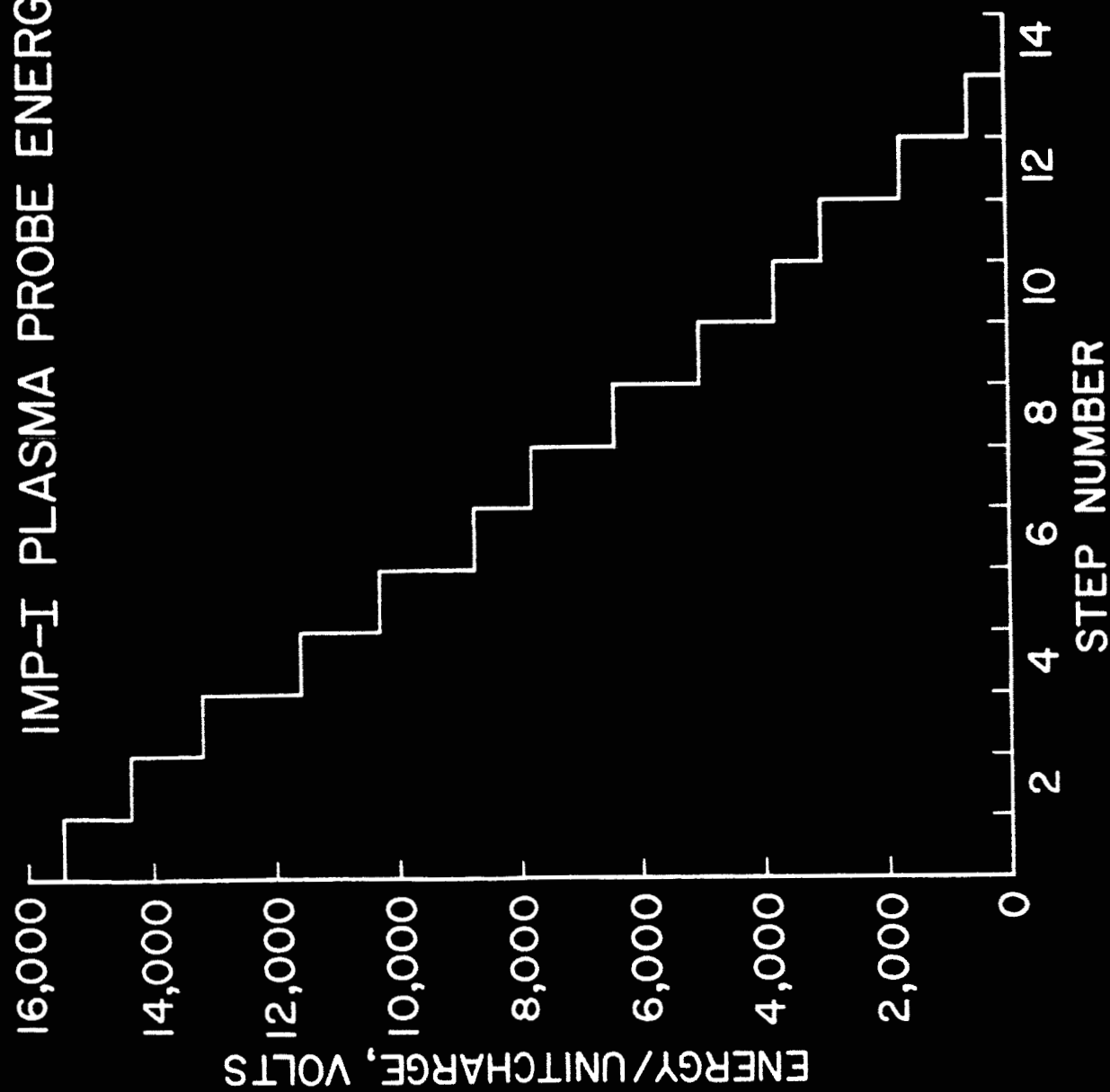


Figure 2.

IMP-I PLASMA PROBE CONFIGURATION

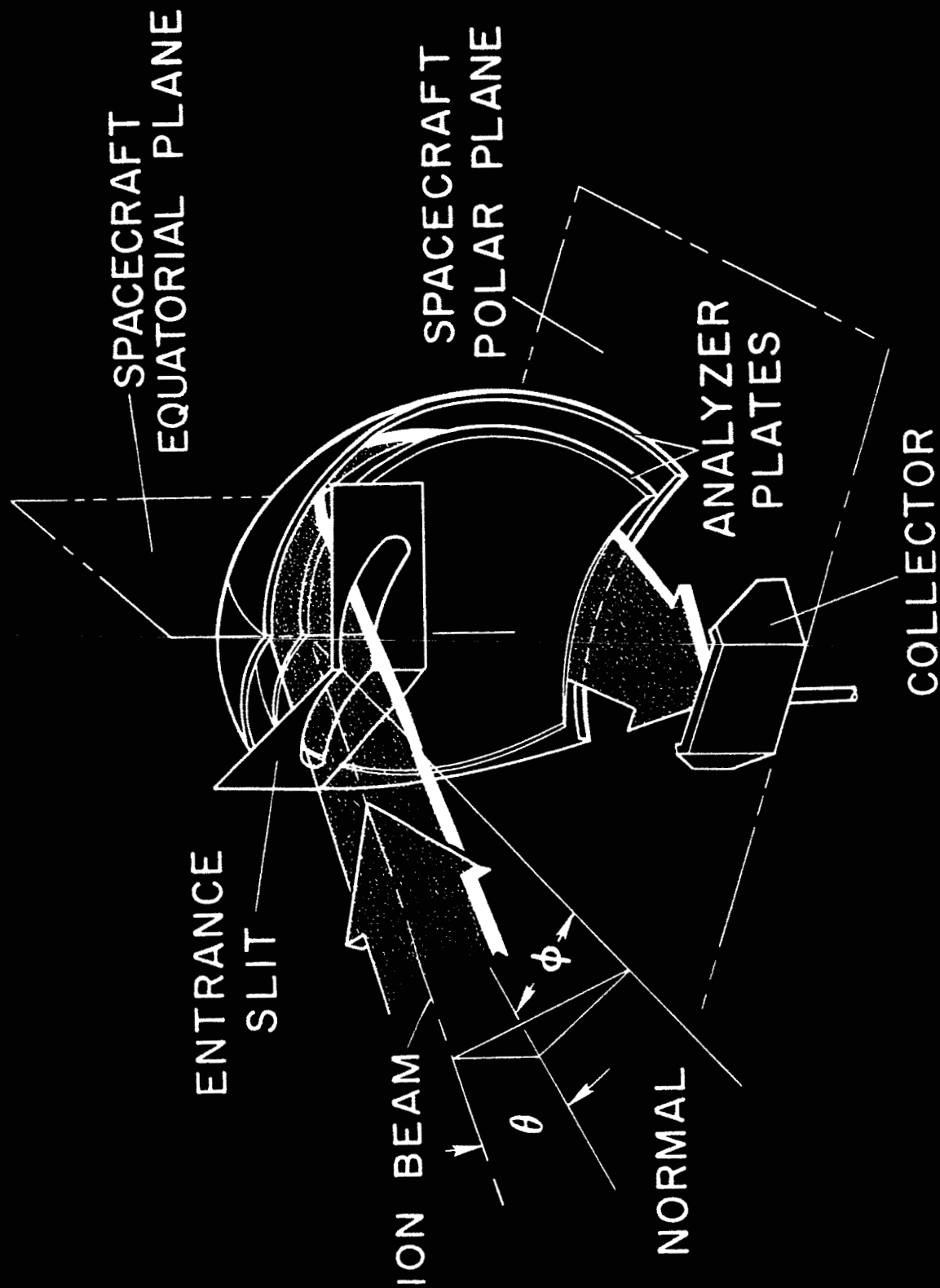


Figure 3.

IMP-I PLASMA PROBE ϕ ACCEPTANCE

$\theta = 0^\circ$
ENERGY STEP NO.13

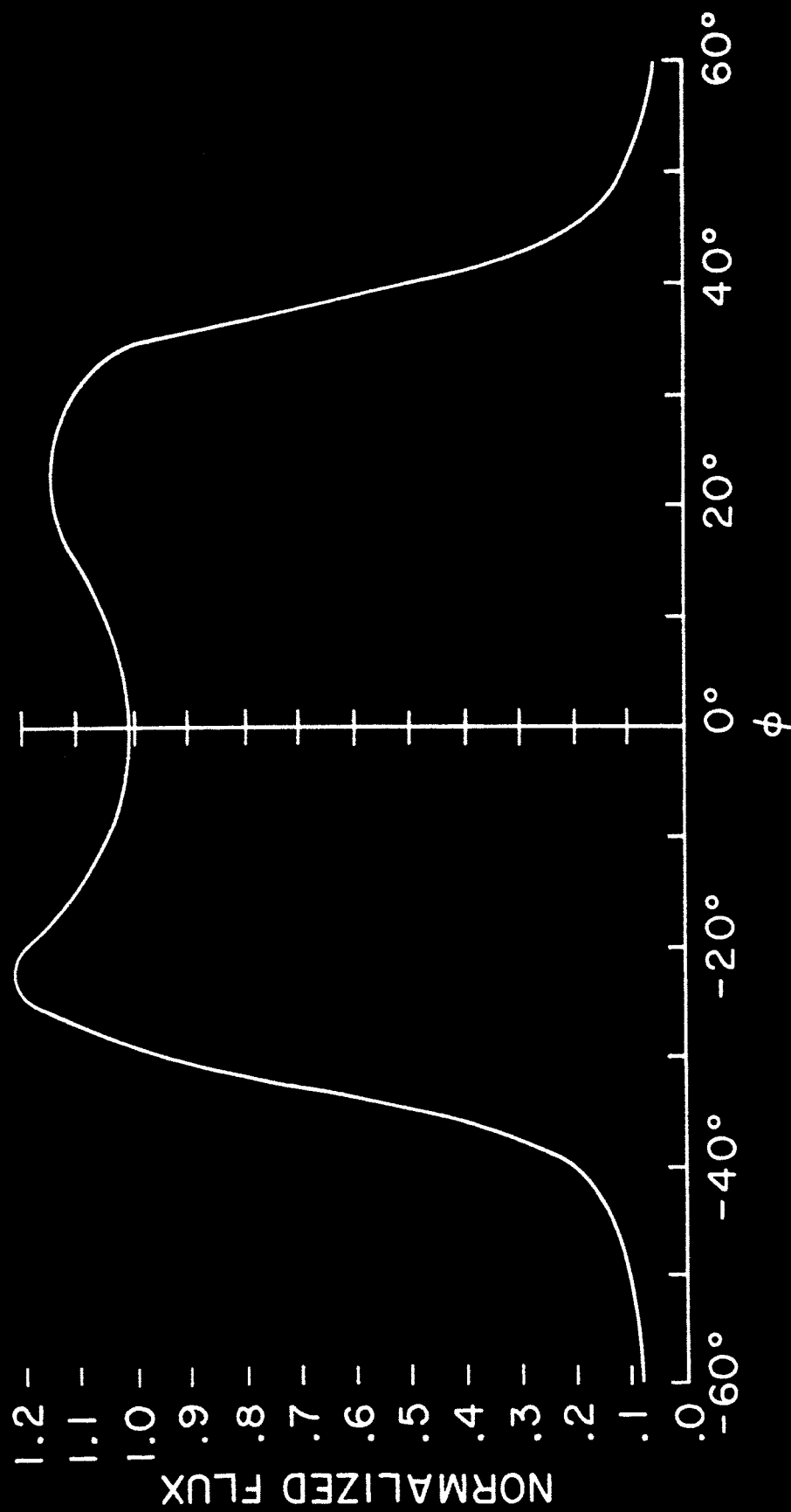


Figure 4.

IMP-I PLASMA PROBE GEOMETRY

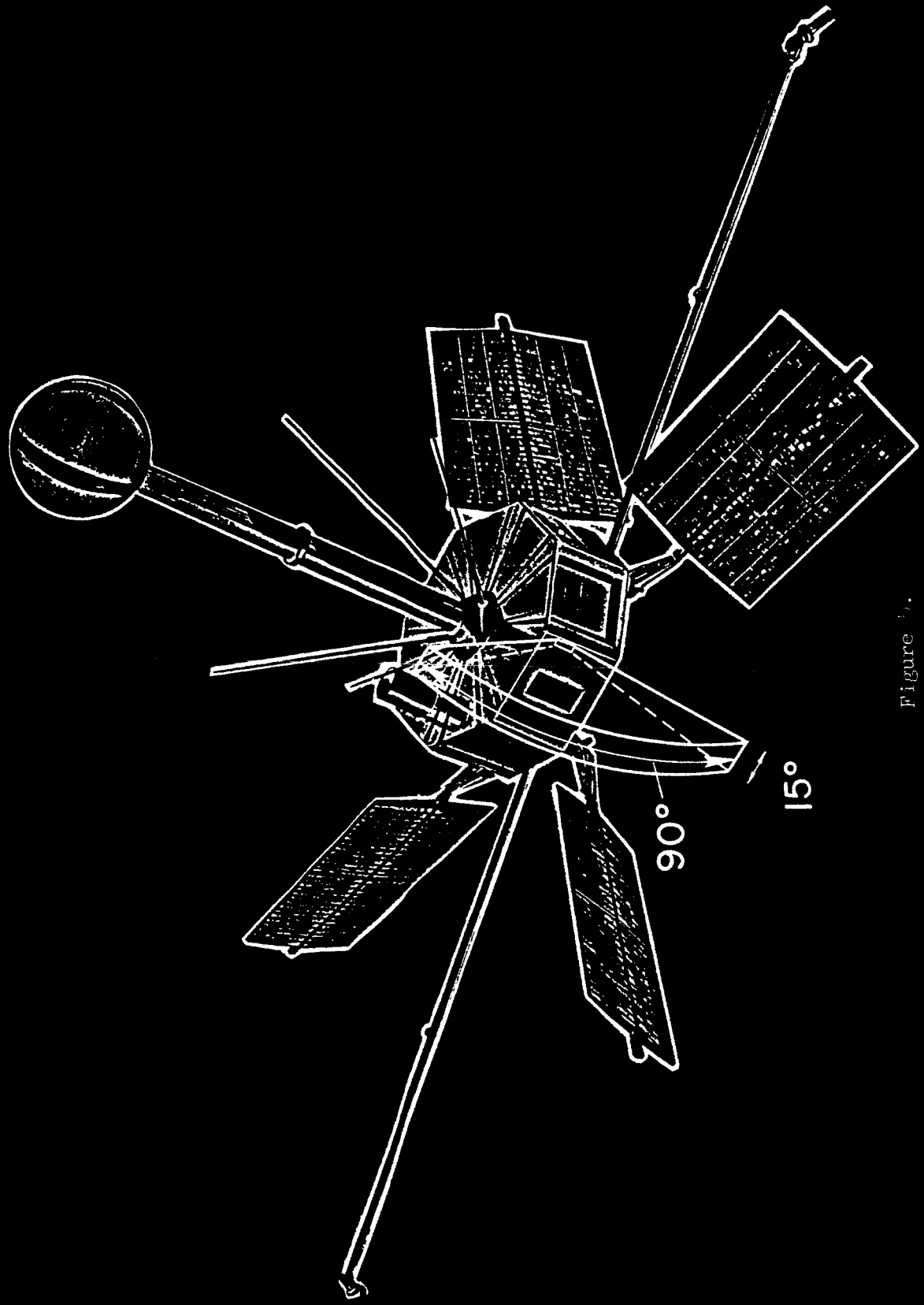
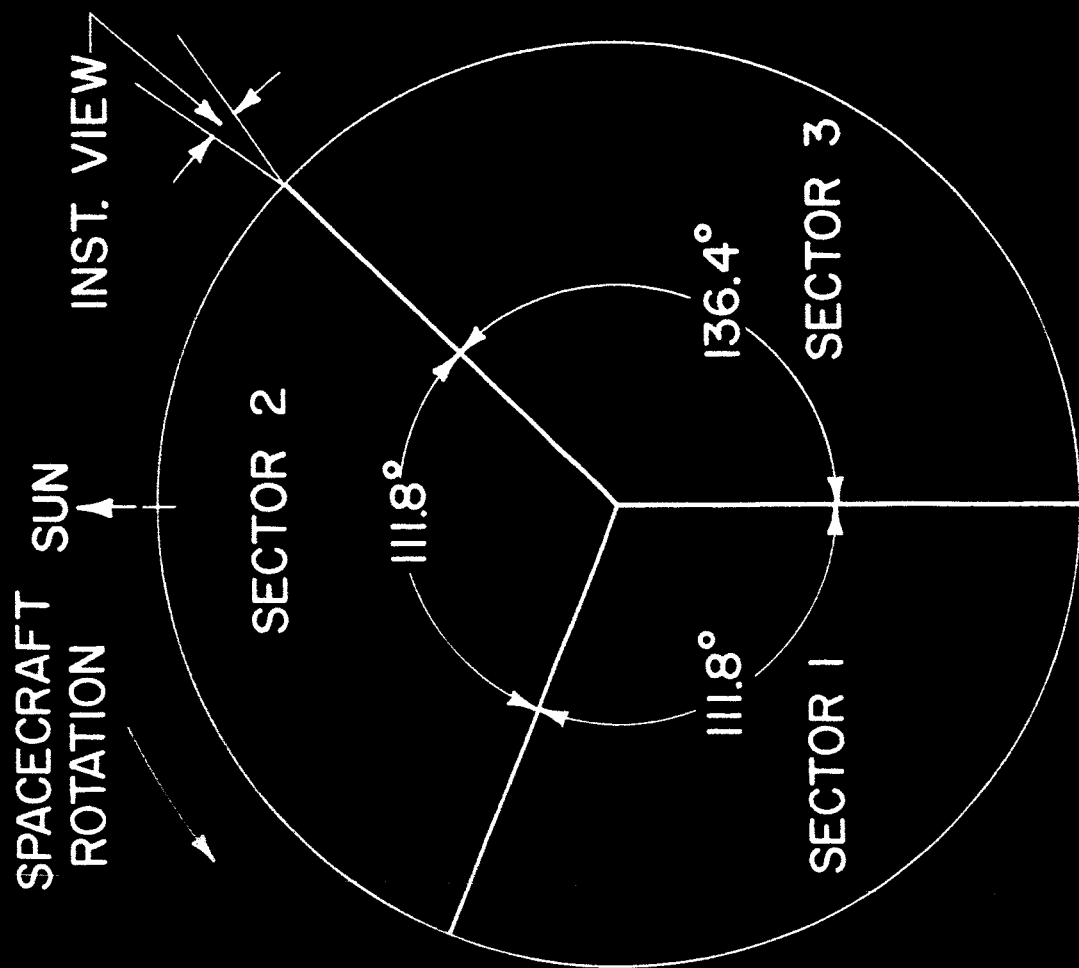


Figure 1.



IMP-I PLASMA PROBE DATA ACQUISITION TIMING DIAGRAM

BASED ON 22.18 RPM
SPACECRAFT SPIN RATE

Figure 6.

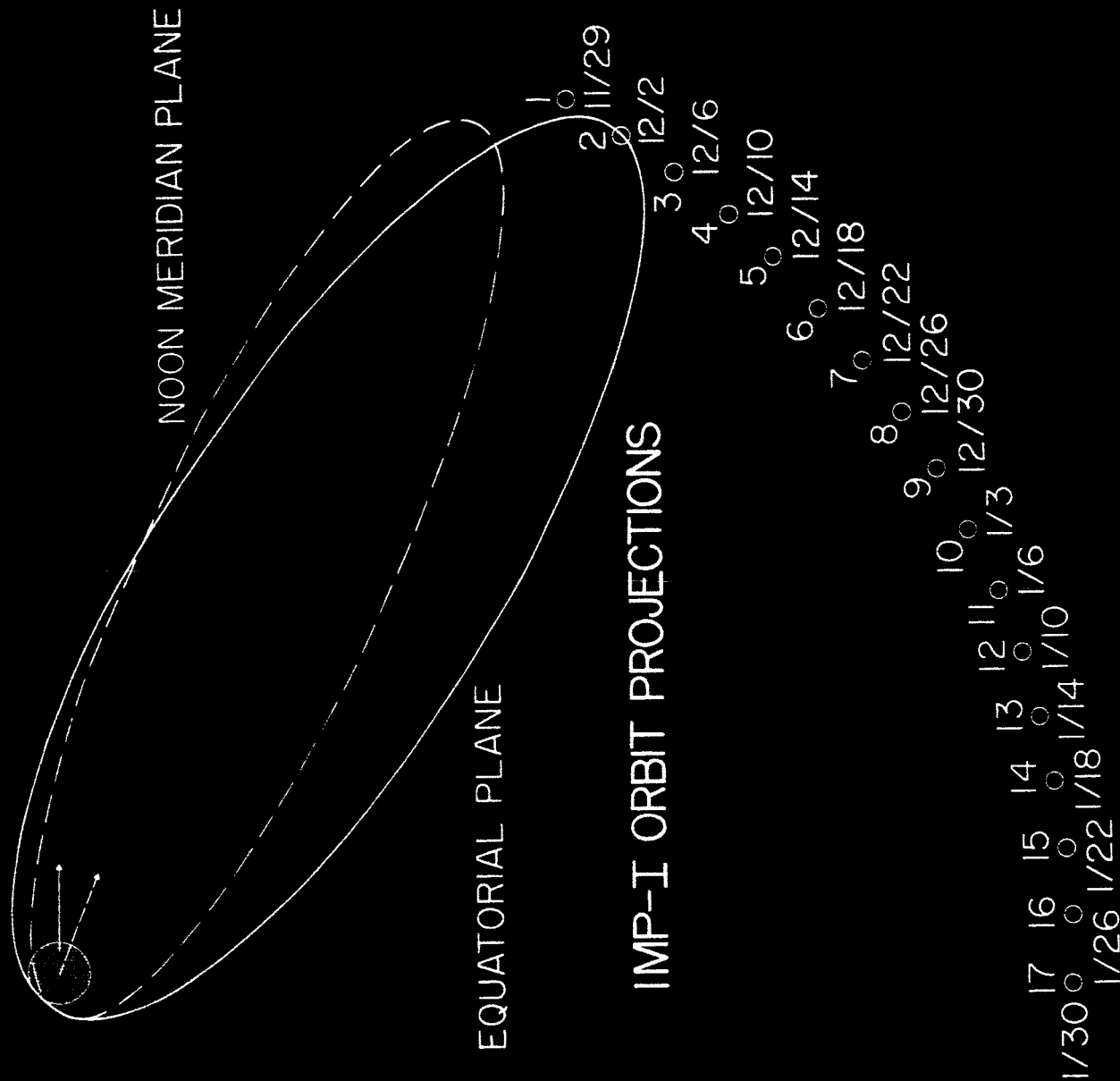
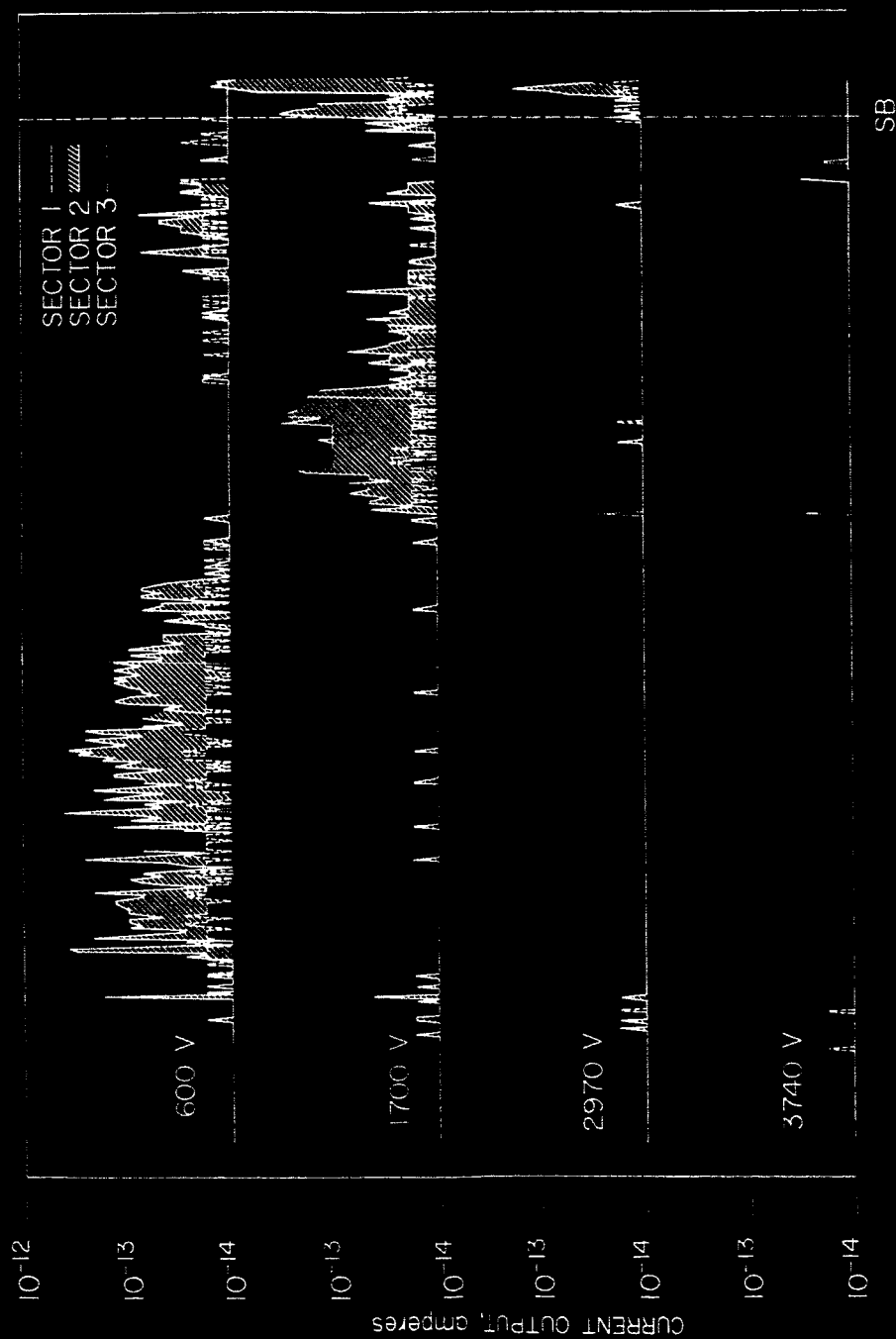


Figure 7.

IMP I PLASMA PROBE OUTPUT

ORBIT 2, 1-2 DEC 63



EARTH
RADII

TIME

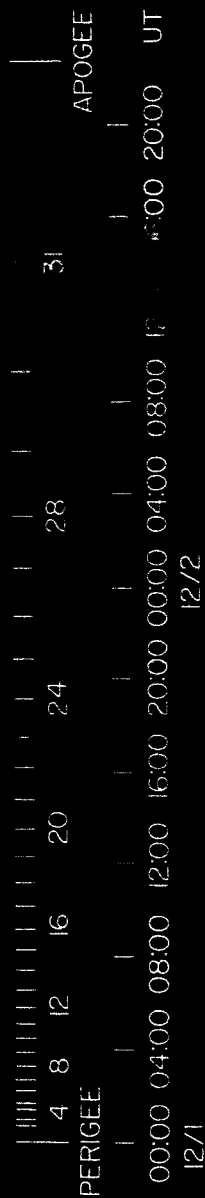


Figure 3.

IMP I PLASMA PROBE OUTPUT

ORBIT 3, 4-6 DEC 63

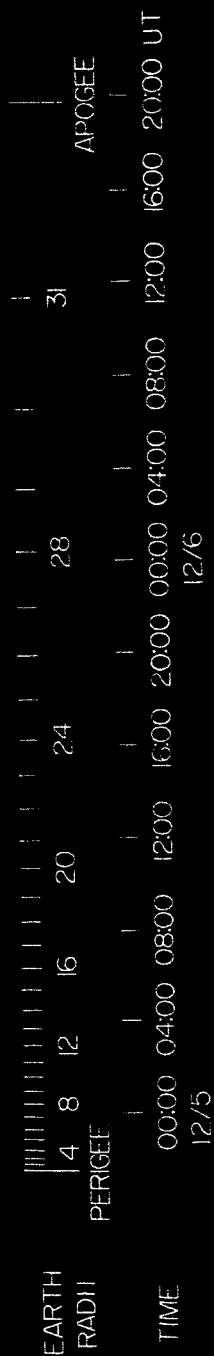
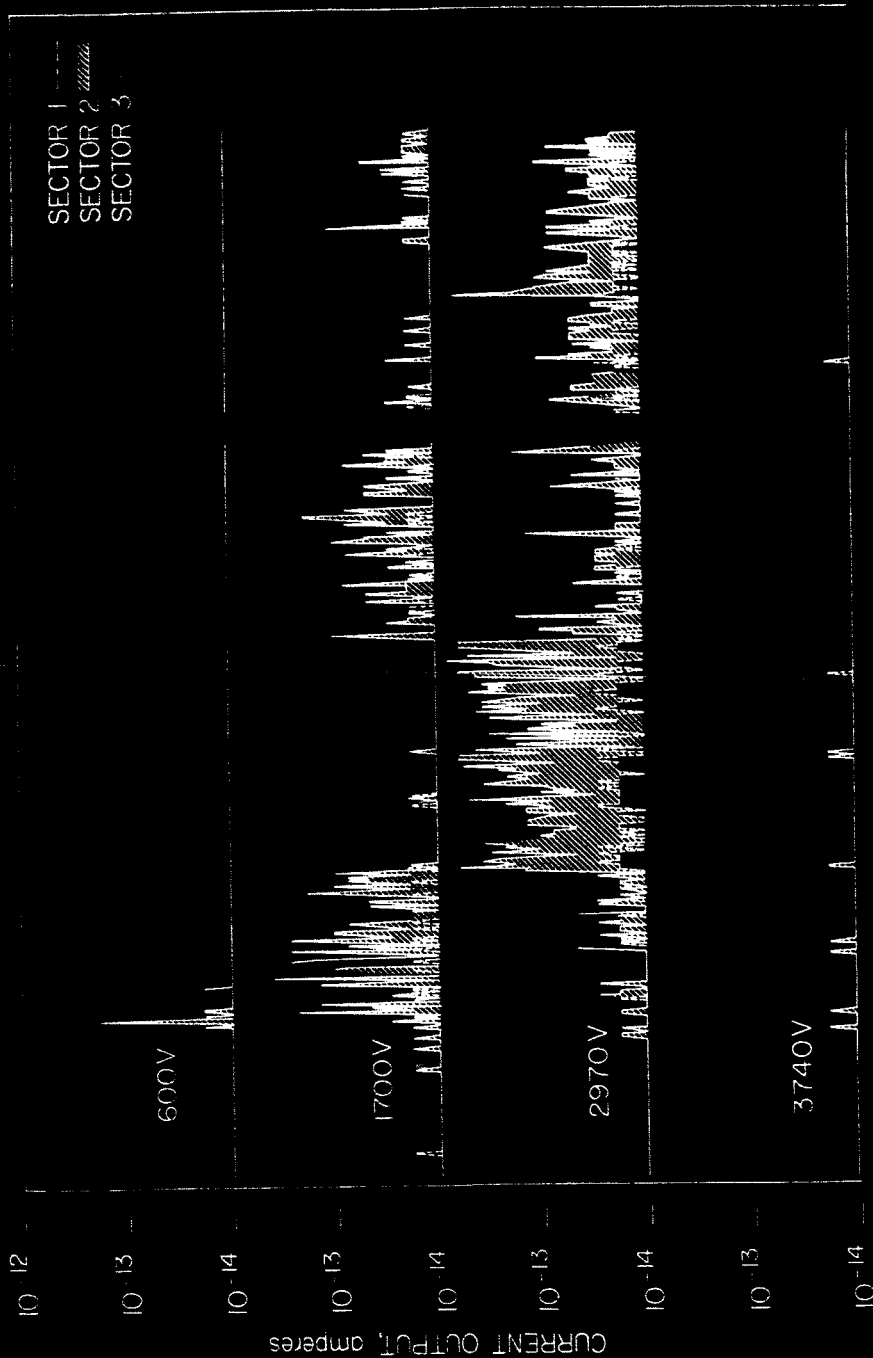
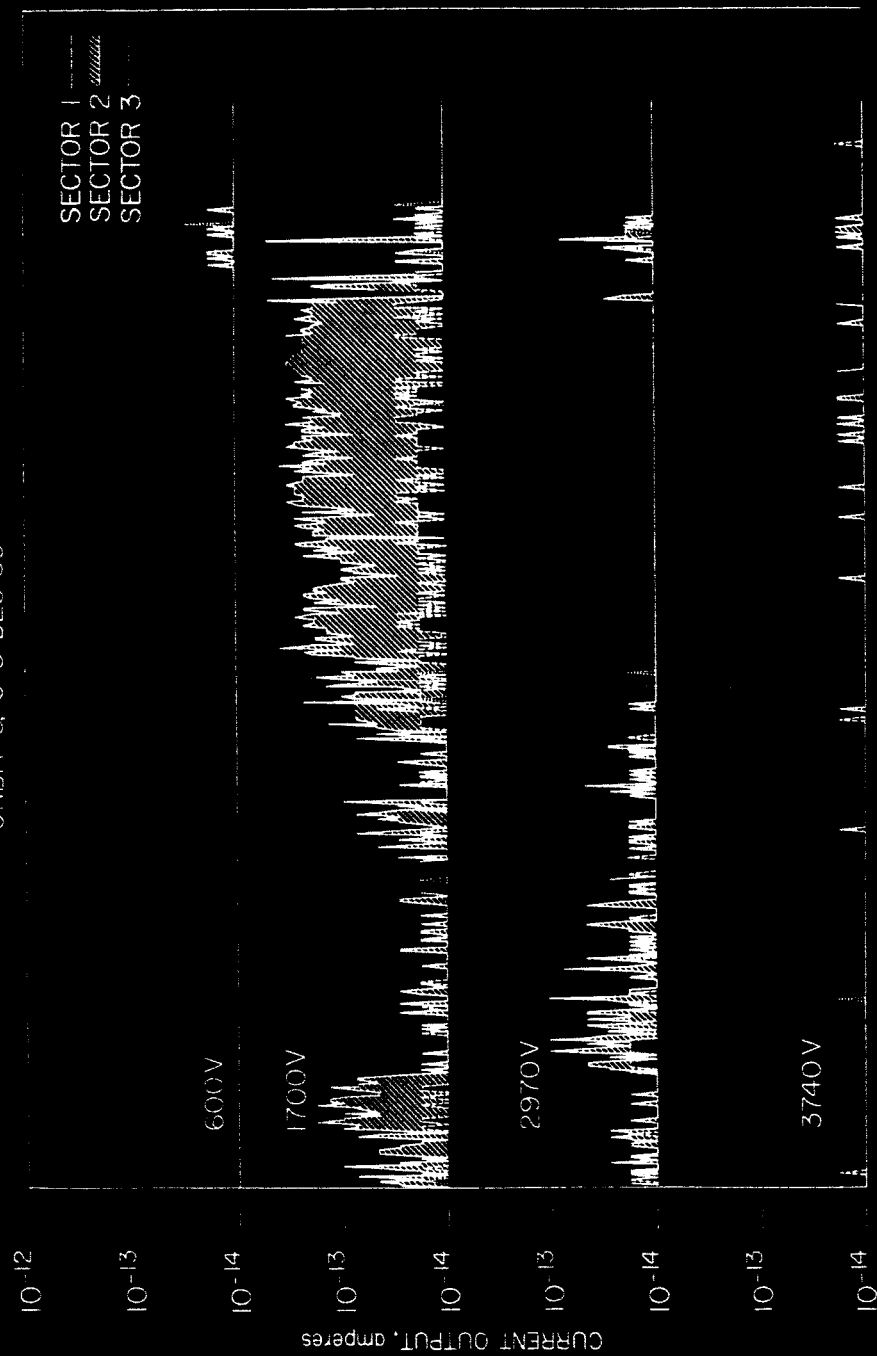


Figure 9.

ORBIT 3, 6-8 DEC 63

EARTH
RADIATION

APOGEE

31

28

55

3

TIME

20:00 00:00 04:00 08:00 12:00 16:00 20:00 00:00 04:00 08:00 12:00 16:00 UT

121

12/8

Figure 10.

IMP I PLASMA PROBE OUTPUT

ORBIT 17, 31 JAN - 1 FEB '64

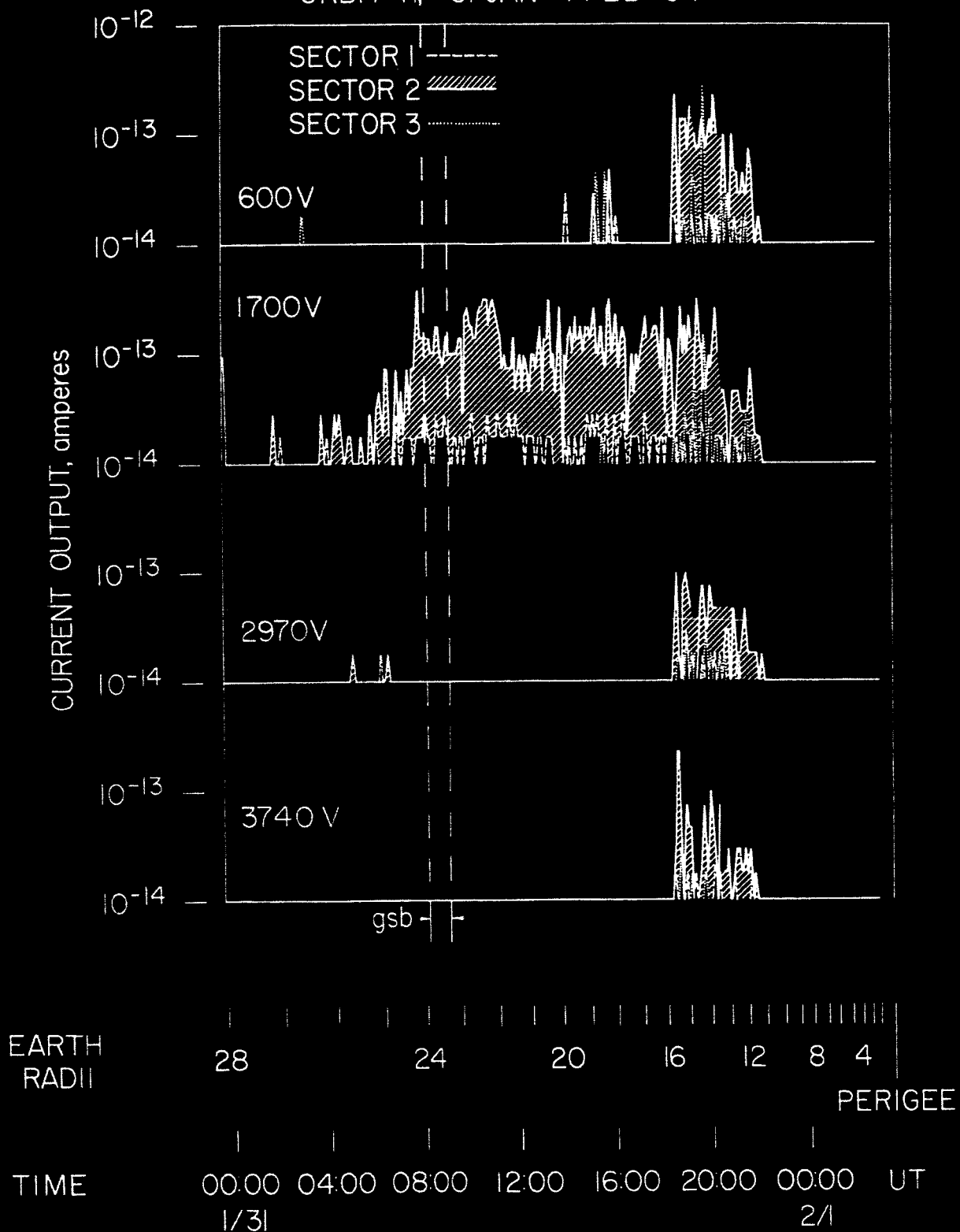


Figure 11.

IMP I PLASMA PROBE OUTPUT

ORBIT 13, 15-16 JAN. '64

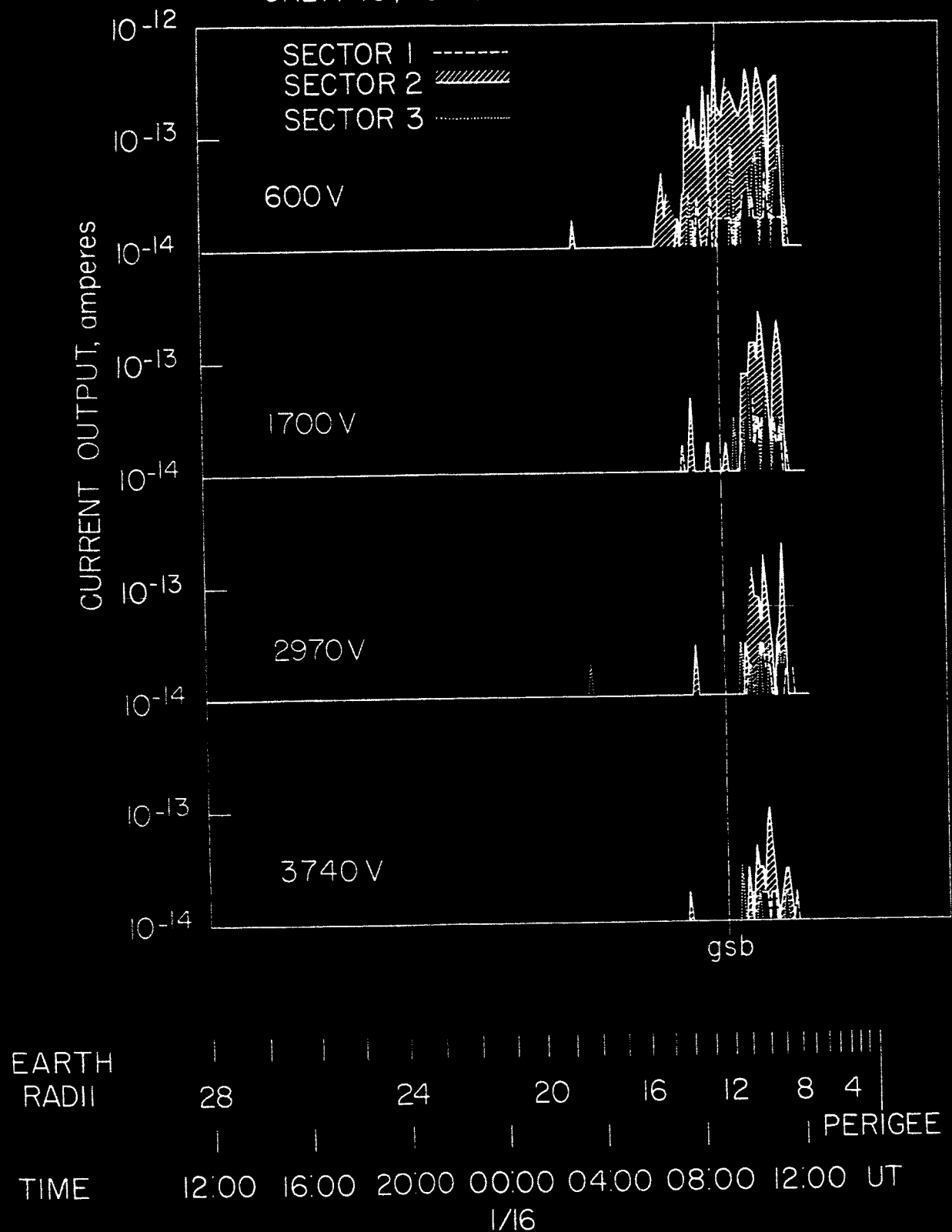


Figure 12.

IMP-I PLASMA PROBE OUTPUT

ORBIT 15, 23-24 JAN '64

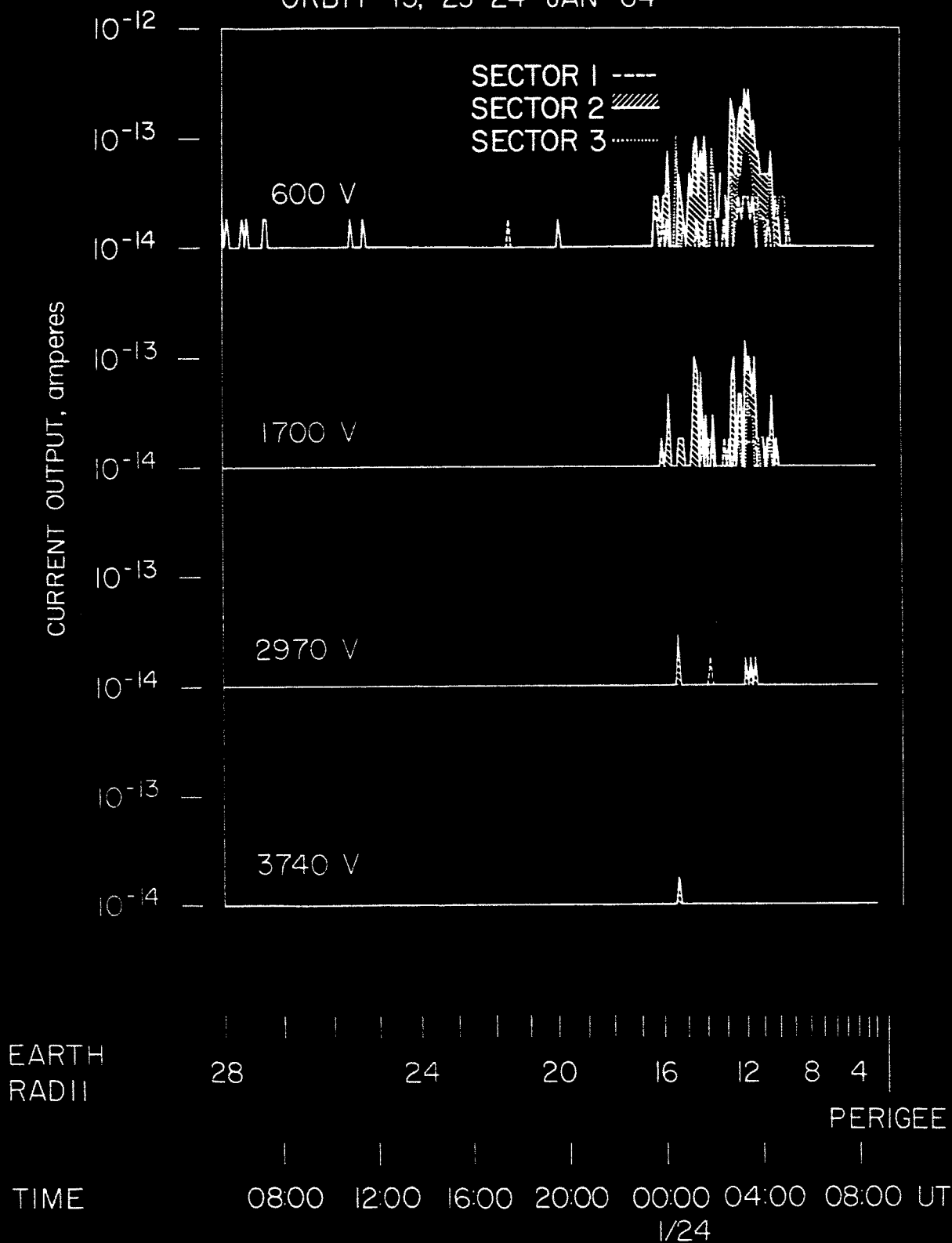


Figure 13.

IMP-I PLASMA PROBE AVERAGE ENERGY SPECTRUM

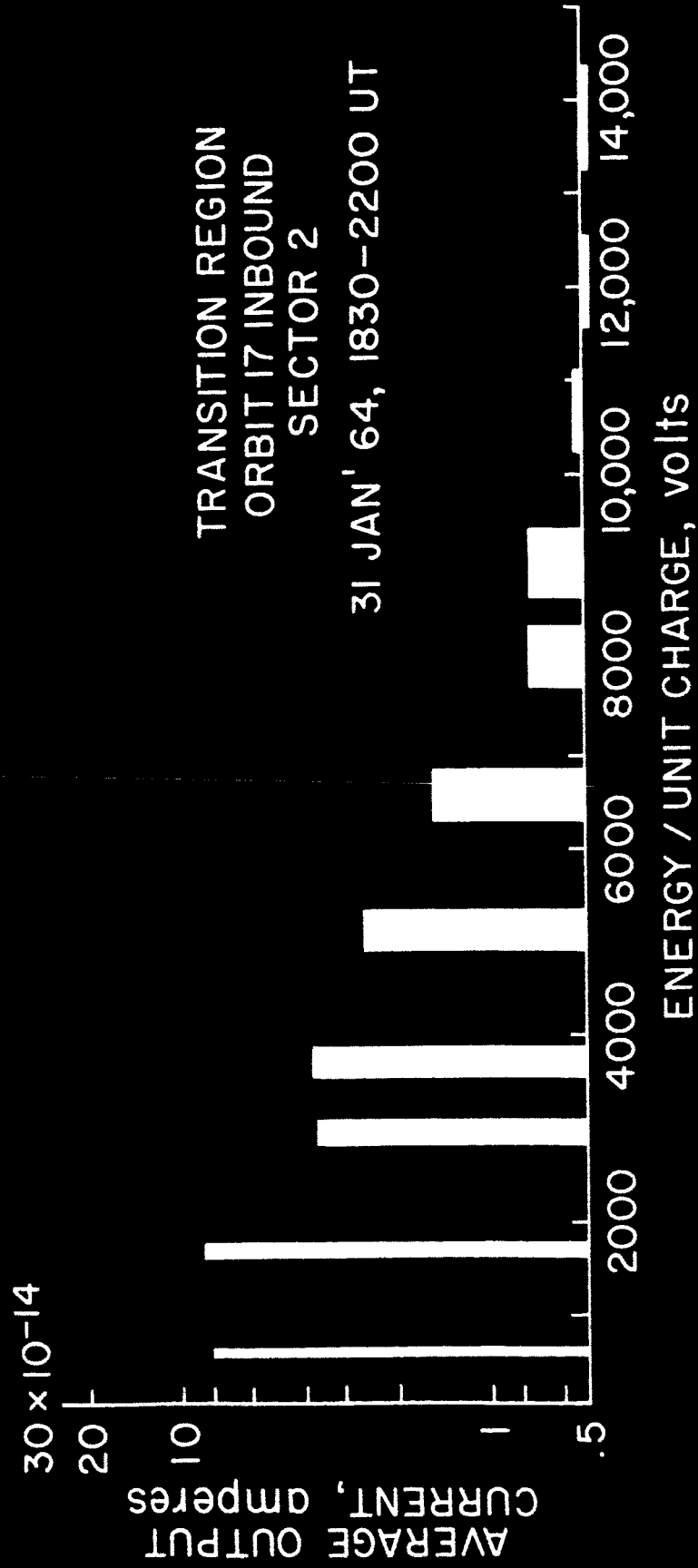


Figure 1b.

IMP-I AMES PLASMA PROBE MEASUREMENTS OF TRANSITION REGION

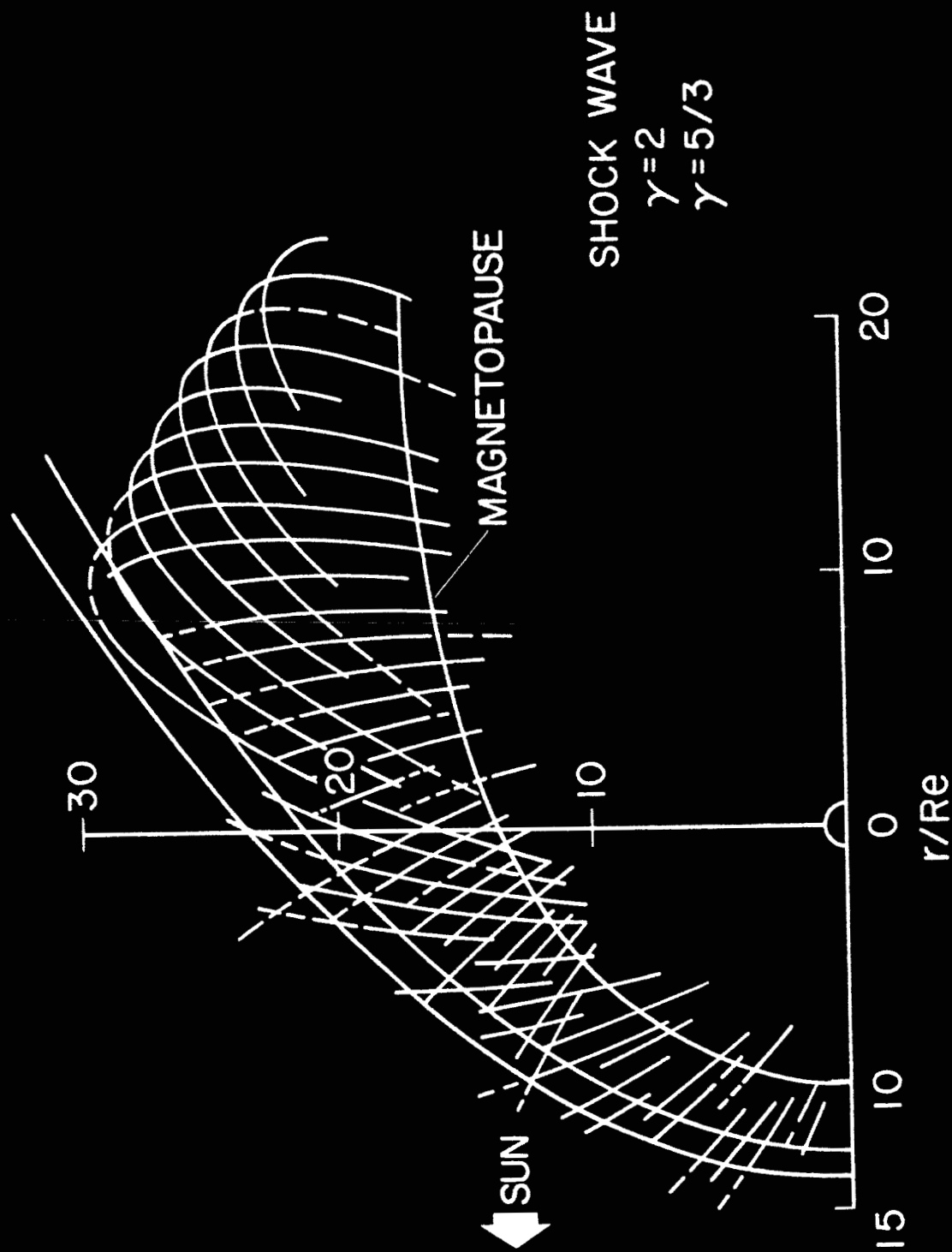


Figure 15.

ROTATED BOUNDARY TRAVERSALS

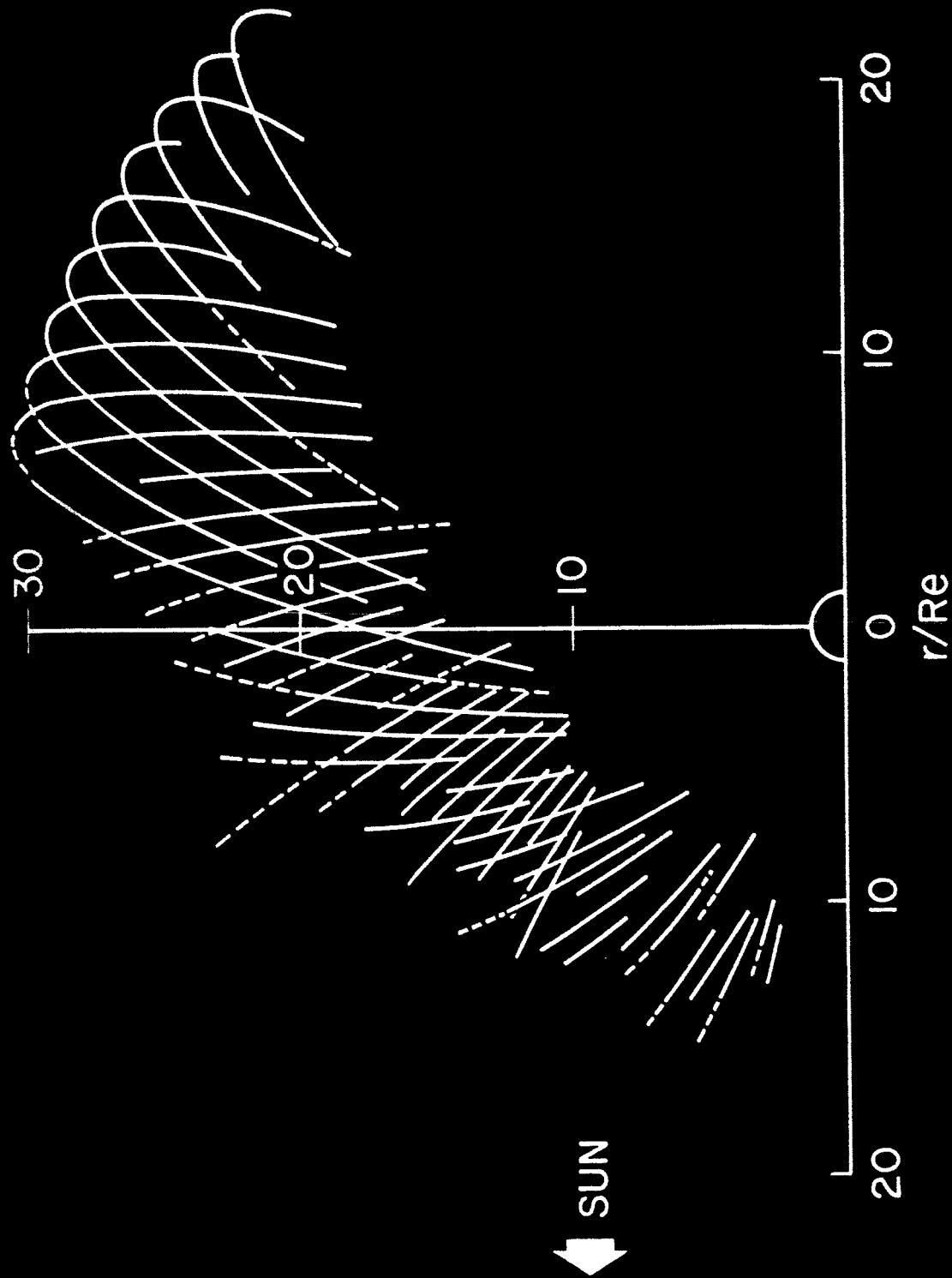


Figure 16.